CALCIUM CARBONATE CRYSTALLIZATION IN THE PRESENCE OF POLYMERIC ADDITIVES

By

Parminder Agarwal

A DISSERTATION

Submitted to
Michigan State University
in partial fulfillment of the requirements
for the degree of

Doctor of Philosophy

Department of Chemical Engineering & Materials Science
&
Department of Chemistry

2002

ABSTRACT

CALCIUM CARBONATE CRYSTALLIZATION IN THE PRESENCE OF POLYMERIC ADDITIVES

By
Parminder Agarwal

Crystallization is one of the most widely used unit operations in the process industries. Impurities and/or additives greatly affect the crystallization process by alteration of nucleation, growth, and even phase transformation kinetics. This study is aimed at the design of additives with the intent of modifying a specific crystallization process.

Calcium carbonate is used industrially for a variety of applications, such as filler for plastic materials, rubber and paper. Precipitation of calcium carbonate on surfaces, also known as scaling, is a major problem for industrial equipment. Therefore, studying the crystallization of calcium carbonate is important from its inhibition as well as its control point of view.

Polycarboxylic acids are good chelating agents and greatly affect calcium carbonate crystallization. Maleimide was used as monomer for synthesis of polymaleimide using anionic and metal oxide-alcohol initiators. The hydrolysis of these polymaleimide resulted in polycarboxylic acid polymers. Proton NMR studies confirmed that the polymers synthesized using different initiators possessed different monomer linkages, with the percent C-N connected monomers lower in the case of metal oxide-alcohol type of initiators (about 40 percent) than for anionic initiation (about 80 percent). Gel permeation chromatography (GPC) was used for molecular weight determination of the polymers. Molecular weight of polymers made by metal oxide-alcohol initiators was about 11500 and was three times the molecular weight of polymers made by anionic

polymerization. The effect of the resulting polymers used as additives in the crystallization of $CaCO_3$ was studied using a variety of techniques. Direct titration using a calcium selective electrode showed that the calcium chelating strength of the polymers was better than some of the commercial detergent building formulations currently in use such as Acusol® and polyaspartic acid. The kinetics of $CaCO_3$ crystallization were studied by nephelometry by monitoring crystal nucleation and growth rates. Polymaleimide synthesized by anionic polymerization was the most efficient inhibitor and exhibited a 59 percent growth rate inhibition at a concentration of 1.4 ppm. Raman spectroscopy was used for *in situ* monitoring of the effect of these additives on polymorph composition during the crystallization. Calcite is thermodynamically the most stable form of $CaCO_3$ and is formed predominantly during the industrial processes for manufacture of precipitated $CaCO_3$. Addition of 1.4 ppm of Acusol® and polyacrylic acid caused the vaterite form to crystallize out exclusively. XRD and SEM data were used to corroborate the Raman data and the results were within two percent of each other.

ACKNOWLEDGMENTS

I thank Dr. Kris A. Berglund for his guidance and invaluable ideas. He kept me focused on my research and helped me go through some of the most testing times of my life. It was his patience and perseverance with me that helped me finish in a timely manner. I also thank him for giving me this unique opportunity to pursue a dual degree in chemistry and chemical engineering. This has helped me look at a comprehensive picture rather than focus on only one aspect.

I would like to thank all those faculty members in chemistry and chemical engineering departments with whom I interacted. I thank the committee members, Dr. Gary Blanchard, Dr. Babak Borhan & Dr. Christian Lastoskie for their time, advice and support.

My manager at Procter and Gamble Pharmaceuticals, Dr. Averrin Mwalupindi helped me get acquainted with working in industry. I am indebted to him for teaching me the problem solving skills and how to work within time limits. I also appreciate the support from Kaiser Optical Inc. and Mettler Toledo for their instrument donations.

A special thanks to all the group members of the Berglund group, past and present, Adam, Al, Carina, Charles, Dale, DeeDee, Dilum, Fang, Hasan, Javier, Jennifer, Johnny, Lili, Matt, Mike, Rosanna and Sri. It was their support that helped me learn various instruments in lab and their ideas and suggestions helped whenever I got stuck in my research.

My friends like Manish, Mahesh, Abhi, Skanth, Kedar, Sanjeev and Reddy had helped me adjust to the life in United States. Thanks for the good time we had together; it was your company that made living several thousand miles away from home even possible.

I cannot thank my family enough; my parents have lived beyond their means to make sure that I get the best of education. It is their faith in me that has made me emerge successful in most difficult times in my life. My wife, Rakhi's contribution cannot be expressed in words. Thank you Rakhi for understanding me, showering your love when I needed it most. It was your efforts that made this work possible!

TABLE OF CONTENTS

LIST OF TABLES

LIST OF FIGURES

Chapter 1

INTRODUCTION

Crystallization is an important unit operation in the chemical industry and is second only to distillation with respect to its applications. The popularity of crystallization is attributed to its cost effectiveness and very high purity of the product obtained. It finds applications in a variety of industries including pharmaceutical, food and fine chemicals. The goals of those employing crystallization are very diverse and can include large crystals with a small crystal size distribution, increasing yield and purity of product, control over the polymorph produced, the effect of additives on crystallization and inhibiting crystallization in select systems. The fundamental understanding of crystallization from solution and efficient process monitoring and control are needed to achieve such goals.

Scaling (crystallization of sparingly soluble inorganic salts) on surfaces is a major problem in the chemical and detergent industries. This problem is particularly acute in systems where surface area is vital such as in boilers, heat exchangers and chillers. In the detergent industry scale prevention is vital in order to provide a good cleansing environment. Therefore, a goal of this research is synthesis of new inhibitors for crystallization. A calcium carbonate batch crystallization system has been used to investigate the effect of presence of additive with respect to the phase of the resulting polymorph.

1.1 Crystallization

The driving force for crystallization is generation of supersaturation. Supersaturation is defined as the difference in the chemical potential between a solution and a solid at the same temperature. The supersaturation governs nucleation and growth kinetics, two of the most important kinetic processes that occur during crystallization.

1.1.1 The role of supersaturation in crystallization

The change in chemical potential for the crystallization process can be written as

$$\Delta\mu = \mu_2 - \mu_1 \tag{1.1}$$

where μ_2 and μ_1 are the chemical potentials at a given temperature of the crystal and the solution, respectively. The negative of this quantity is called the 'affinity of reaction' and makes the driving force a positive quantity.[1] The 'affinity of reaction' is defined as

$$\varphi = -\Delta\mu = \mu_2 - \mu_1 \tag{1.2}$$

The chemical potential μ is defined as

$$\mu = \mu_0 - RT \ln a \tag{1.3}$$

where μ_0 is the standard potential and 'a' is the solute activity.

The supersaturation S can be expressed in dimensionless terms[2] by

$$S = \frac{\varphi}{RT} = \frac{\mu_1 - \mu_2}{RT} \tag{1.4}$$

This equation can be further simplified to

$$S = \nu \ln\left[\frac{a_1}{a_2}\right] = \nu \ln\left[\frac{\gamma_1 c_1}{\gamma_2 c_2}\right] \tag{1.5}$$

where γ_1 and γ_2 are the activity coefficients, c_1 &, c_2 are concentrations of solute in solution and crystal respectively. ν is the number of ions in a molecular unit.

However due to inherent difficulties in measuring the activities, three assumptions are made for approximation of the above formula:

(1) The activity coefficients are assumed to be independent of the concentration for the crystal and the solution so that their ratio is taken as unity.

(2) The number of ions ν is taken to be unity. This reduces equation **(1.5)** to

$$S = \nu \ln\left[\frac{c_1}{c_2}\right] = \ln(S_C + 1) \qquad \textbf{(1.6)}$$

where $$S_C = \left[\frac{c_1 - c_2}{c_2}\right] \qquad \textbf{(1.7)}$$

(3) S_C is taken to be much less than unity therefore equation **(1.7)** reduces to

$$S = S_C = \left[\frac{c_1 - c_2}{c_2}\right] \qquad \textbf{(1.8)}$$

This definition of supersaturation **(1.8)** is the most widely used expression because of the relative ease of measurement. Numerous studies have been undertaken to justify the use of this expression.[3,4] Cooling, anti-solvent addition, chemical reaction and pH change are some of the more commonly used methods to generate supersaturation.

1.1.2 Nucleation

Once supersaturation has been generated in the system, nucleation has to occur for crystallization to proceed. There are two main kinds of nucleation; primary and secondary. Primary nucleation is the assembly of solute molecules into stable nuclei through excess chemical potential. Primary nucleation is homogenous or heterogeneous depending on whether these nuclei are formed in absence or presence of foreign particles, respectively. Secondary nucleation occurs when new crystals are formed in the presence

of growing crystals in solution.[5] Experimental studies have not confirmed a definitive generalized model for nucleation so the following empirical model is used to describe most data:

$$B^\circ = k_N W^i M_T^j (\Delta C^k) \qquad \textbf{(1.9)}$$

Where the nucleation rate B° is proportional to the agitation rate W, in rpm, suspension density M_T, in mass per unit volume and supersaturation ΔC. The exponents i, j and k are the coefficients representing the order of dependence of nucleation rate B° on W, M_T and ΔC respectively. The dependence on agitation, suspension density and supersaturation is realized because most nuclei in an industrial crystallizer are generated by contact with the crystallizer environment.[5]

The induction time for crystallization that is observed in batch crystallization is the period between the generation of supersaturation and the appearance of crystals.[5] This parameter is a measure of how fast the nucleation is proceeding in the system. The induction time is not a fundamental characteristic of the system since it depends on the method of measurement and how it is defined; it is a way to monitor crystallization and to compare various crystallization conditions.

1.1.3 Crystal growth

Numerous theories have been proposed to describe crystal growth,[6,7] including the two dimensional growth model, the Burton Cabrera Frank model and the diffusion layer model. These models provide a theoretical basis for correlation of experimental data for the determination of kinetic parameters.

In general, the models contain too many parameters for estimation and an empirical expression relating growth to the supersaturation is used[5]:

$$G = k_g \ \Delta C^i \qquad \textbf{(1.10)}$$

The exponent i is the apparent order of growth rate and k_g represents the rate constant for this growth rate equation. For most crystallization systems, parameter 'k' in **(1.9)** is larger than parameter 'i' in **(1.10)**; therefore, at high supersaturation nucleation dominates over growth resulting in large numbers of small crystals.

1.2 Calcium carbonate

Calcium carbonate is an important industrial compound and is consumed in large quantities by various chemical industries. It is the most important filler used in the plastic and the paper industry. In the plastic industry it accounts for forty percent of the total filler demand.[8] Apart from being used as filler, it is also used in a variety of applications such as sulfur dioxide scrubbing, glass manufacture, waste treatment and heavy metal complexation. Another very important area of research on calcium carbonate crystallization is its inhibition.[9] This is particularly important in the detergent industry, where prevention of scaling (precipitation of inorganic salts, primarily calcium carbonate) is a pre-requisite for good cleansing action of the detergent. Scaling is also a major problem for industrial equipment such as boilers, heat exchangers, chillers etc. where clean surfaces are critical to performance. Therefore, the goals of the current research could be divided into two broad categories as shown in Table 1.1. For the production of calcium carbonate, fast production cycle is desired so small induction time (time between generation of supersaturation and appearance of crystals) and fast kinetics is desired. Although nucleation kinetics should be low in this case because slower

nucleation rate gives smaller number of growing crystals at any moment in time, this gives small number of large crystals, which is usually desired. For inhibition applications, large induction time and slow kinetics is desired to have minimal scaling.

Aspect of Crystallization	**Calcium Carbonate Production**	**Anti-scaling Application**
Induction Time	Small	Large
Nucleation Rate	Small	Zero
Growth Rate	High	Low
Polymorph Kind & Crystal Size	Controlled	-

Table 1.1 Goals of the crystallization experiments for production applications and for crystallization inhibition application.

1.3 Crystallization of polymorphs

1.3.1 Importance of studying polymorphs

Polymorphism is existence of two or more different crystal packing structures of the same molecule. The importance of studying the various polymorphs of any system under investigation is underlined by the differences in their properties. Polymorphs differ in crystal packing and therefore physical properties such as molar volume, density, refractive index and conductivity are also different. The difference in their spatial environment causes the polymorphs to have different spectroscopic properties as seen with infrared (IR), uv, nuclear magnetic resonance (NMR) and Raman measurements. Polymorphs also differ in mechanical properties such as hardness and tensile strength. Kinetic and thermodynamic properties like solubility, reaction rate, melting temperature and enthalpy are also unique to the kind of polymorph present. These differences in properties motivate scientists and engineers[5,10] in the development of control schemes for polymorph production.

1.3.2 Calcium carbonate polymorphs

Calcium carbonate used in industrial applications is classified on the basis of its source. Ground calcium carbonate (GCC) results directly from the mining process.[11] The production process maintains the calcium carbonate very close to its original state. GCC is primarily the calcite polymorph, which is thermodynamically the most stable form at room temperature.

Precipitated calcium carbonate (PCC) is produced through the recarbonization process or as a by-product of chemical processing[11] such as the Solvay method or caustic soda production. Current industrial processes form predominantly the calcite polymorph; however, PCC can produce other polymorphs and morphologies. The current research is relevant to control of the polymorph formed during the production of PCC.

Calcium carbonate exists as three different polymorphs: calcite, aragonite and vaterite. Scanning electron microscope (SEM) images of these three polymorphs are shown in Fig. 1.1 and a comparison of their properties is given in Table 1.2. From the data shown in Table 1.2, it is evident that the vaterite and aragonite forms would perform better in various applications, such as filler in plastic and paper industry due to their lower specific gravities, which would give more volume for same weight. Mechanical properties such as hardness are also better for these polymorphs. Use of these polymorphs as filler in the paper industry would give a better quality paper due to their stronger luminescence and better refractive index. Aragonite form is metastable and only formed at high temperature of around 100°C.

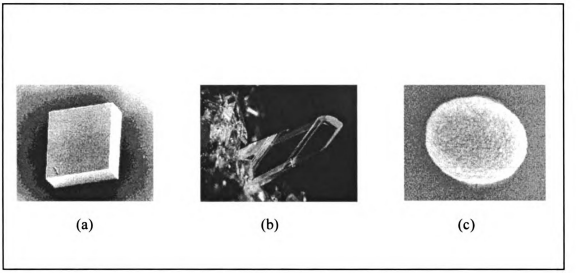

Figure 1.1 Scanning electron micrographs of calcium carbonate polymorphs.

(a) Calcite (b) Aragonite (c) Vaterite

Adapted from http://mineral.galleries.com.

Property	*Calcite*	*Aragonite*	*Vaterite*
Crystal Structure	Rhombohedral	Orthorhombic	Hexagonal
Color	White to Pale Yellow	White/Transparent	White/Transparent
Hardness (Mohs)	2.5-3.0	3.5-4.0	3.0-3.2
Specific Gravity	2.7	2.9	2.54
Refractive Index	1.49-1.66	1.7-1.8	1.55-1.65
Luminescence	Weak	Strong	Strong

Table 1.2 Comparison of physical properties of calcium carbonate polymorphs.

Compiled from *http://mineral.galleries.com* and Handbook of Chemistry & Physics, CRC Press, 1971.

1.4 Monitoring of polymorphs during crystallization

A variety of techniques are available for polymorph identification. Infrared spectroscopy (IR), Raman spectroscopy, solid state NMR, powder x-ray diffraction (XRD) and thermal techniques such as differential scanning calorimetry (DSC), thermogravimetric analysis (TGA) have been used for this application;[16,17] however, with the exception of IR and Raman spectroscopy, these techniques cannot be used for *in situ* measurements.

Raman spectroscopy, coupled with a fiber optic probe has advantages over the IR technique for such measurements.[12] One of the main considerations for *in situ* measurements is the ability of the technique to be able to monitor changes in the presence of the solvent that is being used. The systems under consideration use water as the solvent, however water has strong IR absorption and therefore masks some very useful peaks of the carbonate ion. Raman scattering from water is weak[13,14] and the use of this technique avoids problems associated with measurements with monitoring aqueous systems under investigation. The current study uses Raman spectroscopy for *in situ* monitoring of phase transformations during calcium carbonate crystallization.

1.4.1 Raman spectroscopy

When a beam of monochromatic light in the visible region is incident upon a sample that does not absorb light of that wavelength, the light is transmitted. However a very small fraction is scattered in all directions. The intensity of this scattered light is measured in Raman spectroscopy. The line corresponding to incident frequency is known as *Rayleigh line.* The other weak lines observed in the spectra are known as *Raman lines.* The differences between the frequencies of the *Rayleigh line* and the *Raman line* are known as *Raman shifts.* A change in polarizability of the molecule during the vibrational or

rotational motion forms the basis for Raman spectroscopy. The *Rayleigh line*, therefore has the same frequency ν_0, as that of the incident light. The *Raman lines* at frequencies less than ν_0 are known as *Stokes lines* and those having frequencies greater than ν_0 are known as *anti-Stokes lines.* The intensities of *Stokes lines* are greater than intensities of *anti-Stokes lines* by virtue of the Boltzmann distribution. The basis of *Stokes & anti-Stokes* scattering is shown below.

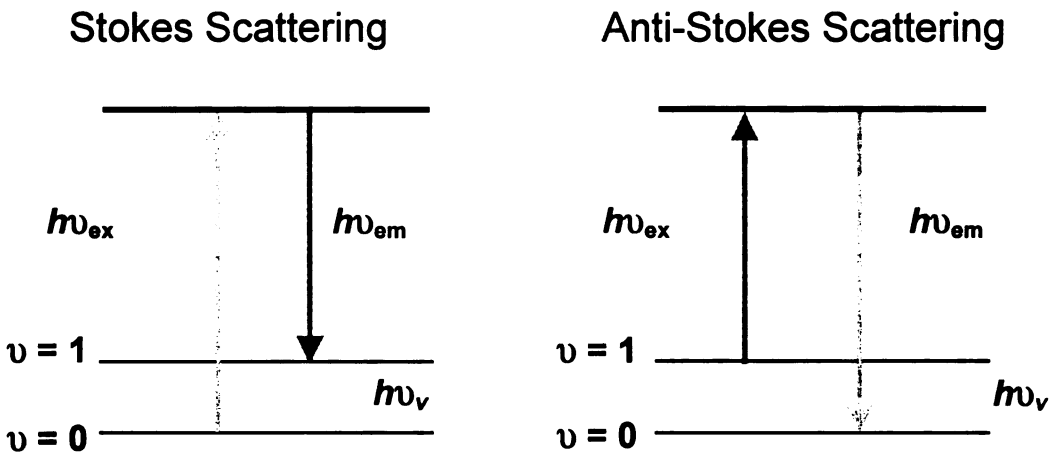

The remote sensing capability of Raman spectroscopy is excellent. All one needs is a fiber optic cable connecting the probe and the spectrometer, this cable can be as long as couple of hundred meters.[15] There are several methods used by researchers to quantify the relative amount of various phases by Raman spectroscopy. The most common are the peak intensity method, the peak position method and the peak intensity ratio method.[16,17] The peak intensity and peak position methods can sometimes be dependent on the experimental conditions such as intensity of the laser and accuracy of calibration. Therefore, peak intensity ratio method has been used for current study.

1.5 The influence of additives on crystal shape

The physical appearance of a crystal is its habit. Although the crystals formed in any process could be classified according to one of the crystallographic systems listed in Table 1.3, the relative sizes of the faces of a particular crystal can vary considerably. This variation is called habit modification.

Form	*Faces*	*Edges*	*Corners*	*Edges at a Corner*	*Elements of Symmetry*		
					Center	*Planes*	*Axes*
Regular Solids							
Tetrahedron	4	6	4	3	No	6	7
Hexahedron	6	12	8	3	Yes	9	13
Octahedron	8	12	6	4	Yes	9	13
Semi-regular Solids							
Truncated Cube	14	36	24	3	Yes	9	13
Truncated Octahedron	14	36	24	3	Yes	9	13
Cubo-octahedron	14	24	12	4	Yes	9	13

Table 1.3 Properties of some regular and semi-regular forms found in crystalline state.

Adapted from "Crystallization" 3rd edition by J. W. Mullin.

1.5.1 Crystal habit

The crystal habit can be controlled by either thermodynamic or kinetic factors. Crystals grown at a very slow rate are usually thermodynamically controlled. In 1878, Gibbs proposed that the total free energy of a crystal in equilibrium with its surroundings at constant temperature and pressure would be a minimum for a given volume.

$$d\,({}_1\Sigma^n A_n \gamma_n) = {}_1\Sigma^n \gamma_n\, d\,(A_n) = 0 \qquad \textbf{(1.11)}$$

where A_n is the area of the n^{th} face. In 1901, Wulff stated that crystal faces would grow at rates proportional to their respective surface energies, where the equilibrium shape is determined by the ratio[18] of the distance from the face, h_n to the specific surface energies, γ_n. A schematic representation of this equilibrium shape is shown in Figure 1.2.[19]

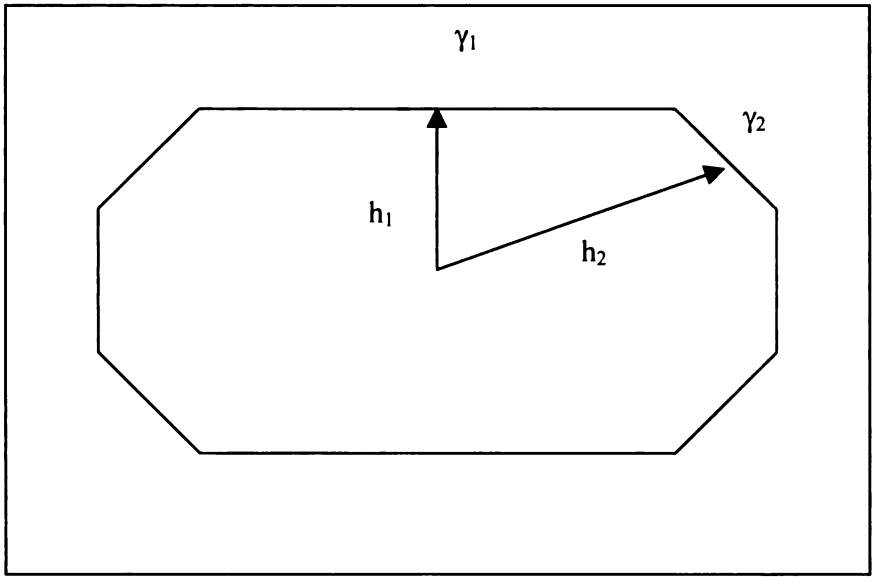

Figure 1.2 Wulff's theorem describes the crystal shape, $\gamma_1 < \gamma_2$.

Adapted from "Crystallization" 3rd edition by J. W. Mullin.

Hartman & Perdok developed a morphological theory that related bond energies to internal structures of crystal morphology.[20] They theorized that crystal growth is controlled by the formation of strong bonds between crystallizing particles called periodic bond chains (PBC). Growth layers of the periodic bond chains form three different crystal faces as shown in Figure 1.3. The F-face (flat) is the elementary face that grows slice after slice and is parallel to at least two PBC vectors. The S-face (stepped) is parallel to at least one PBC vector. The K-faces (kinked) are not parallel to any PBC vector and need no nucleation for growth. The rougher S- and K-faces grow very quickly and are rarely observed. On the other hand, the growth velocity of the F-face is very slow. Thus, the crystal habit is usually dominated by the F-face.

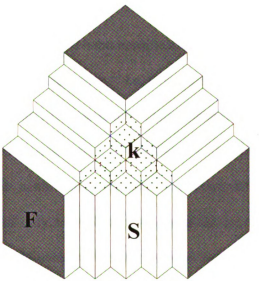

Figure 1.3 Three main types of possible faces of a three-dimensional crystal.
Flat face (F), step face (S) & kink face (K)[21]
Adapted from "Crystallization" 3rd edition by J. W. Mullin.

1.5.2 Effect of additive on habit modification

The crystals may grow more slowly in one direction due to adsorption of additive on specific faces. Thus, an elongated growth of the prismatic habit gives a needle-shaped crystal (acicular habit)[22] and a stunted growth gives a flat plate-like crystal (tabular, plate or flake habits)[22], this is also shown in Figure 1.4.

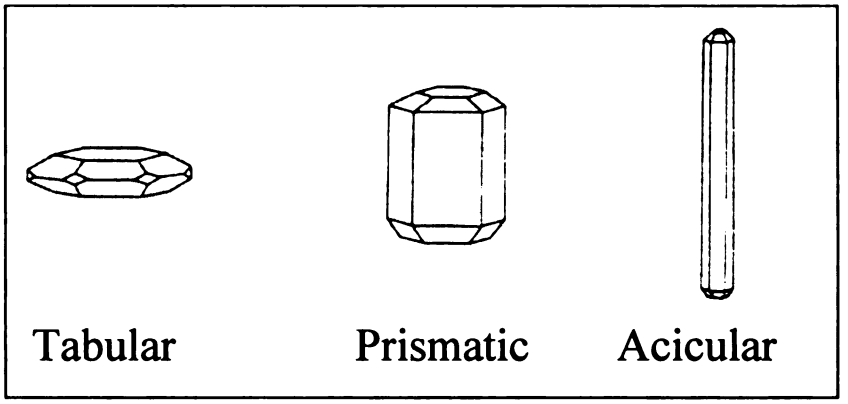

Figure 1.4 Effect of crystal habit modification on hexagonal crystal.

Growth proceeds mostly through kinks,[23] i.e. defects, so blocking these sites is sufficient to hinder crystal growth. In some cases the adsorption that blocks the sites is irreversible. In other cases, however, adsorption of additives is temporary and reversible. The oncoming growing units continuously repulse the additive molecules to the front of faces in growth. Blockage of only a few kinks can cause the growth rate to slow by several orders of magnitude.[24] Additives can be very active at low concentrations.

1.6 Polycarboxylic acid polymers in the detergent industry

Efficient detergent cleansing action requires that scaling or precipitation of insoluble inorganic salts be prevented. Hardness of water is primarily due to calcium and magnesium ions; therefore, one mode of action of detergent additives is chelation with these metal ions and prevention of precipitation. Organophosphates were used for a long time in the detergent industry for their role as anti-scaling and anti-redeposition agents. However, the phosphate content of these detergents caused eutrophication of water bodies. This problem was particularly severe because of the very long biodegradation time associated with these organophosphates. Acrylic acid based polymers and copolymers are being used currently for such applications. Figure 1.5 shows the structures of various polymers used in the detergent industry.[25] Even though these polyacrylic acids do not cause eutrophication, they still possess a long biodegradation time, thereby tending to accumulate in the environment. The long-term effects of this accumulation have not been determined. Very recently, polyaspartic acid polymers have been introduced for such applications due to their shorter biodegradation time.

A number of schemes have been used to synthesize polysuccimide such as catalytic ring closure of aspartic acid or maleamic acid with ring opening by hydrolysis to produce polyaspartic acid. Details of these routes are shown in Figure 1.6. In the current research maleimide was used as the starting point for polyaspartic acid polymer synthesis and the resulting polymers can also be called polymaleimide. The efficiency of these polymers as detergent builders would be determined by comparison with polyacrylic acid and polyaspartic acid.

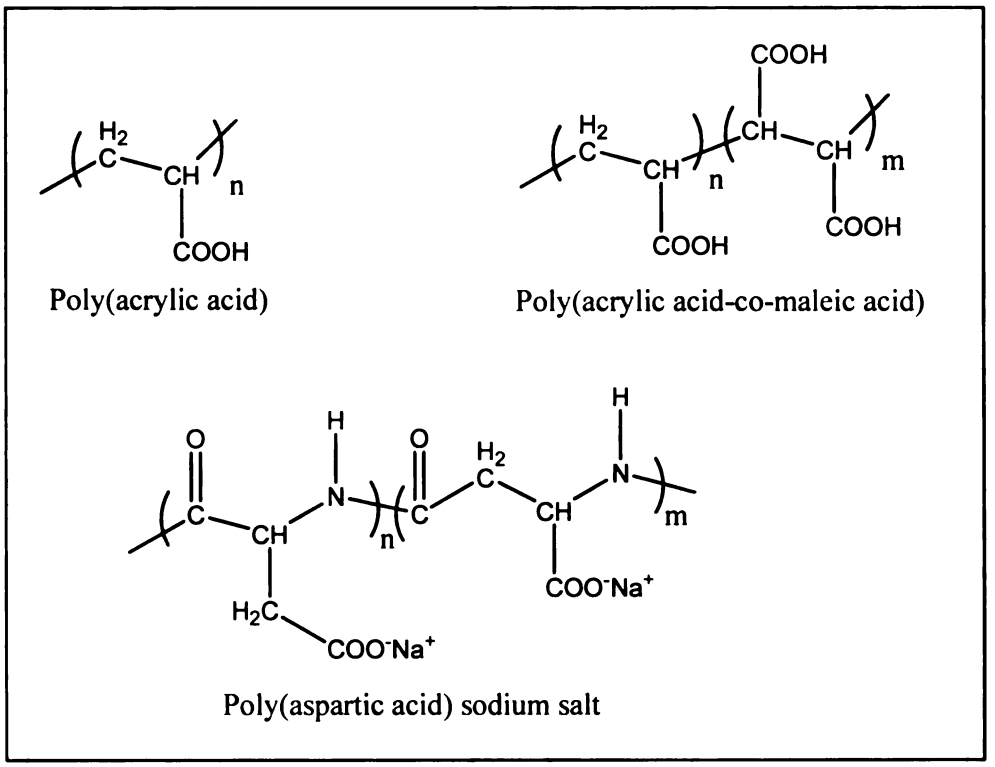

Figure 1.5 Polymers used in the detergent industry. [25]

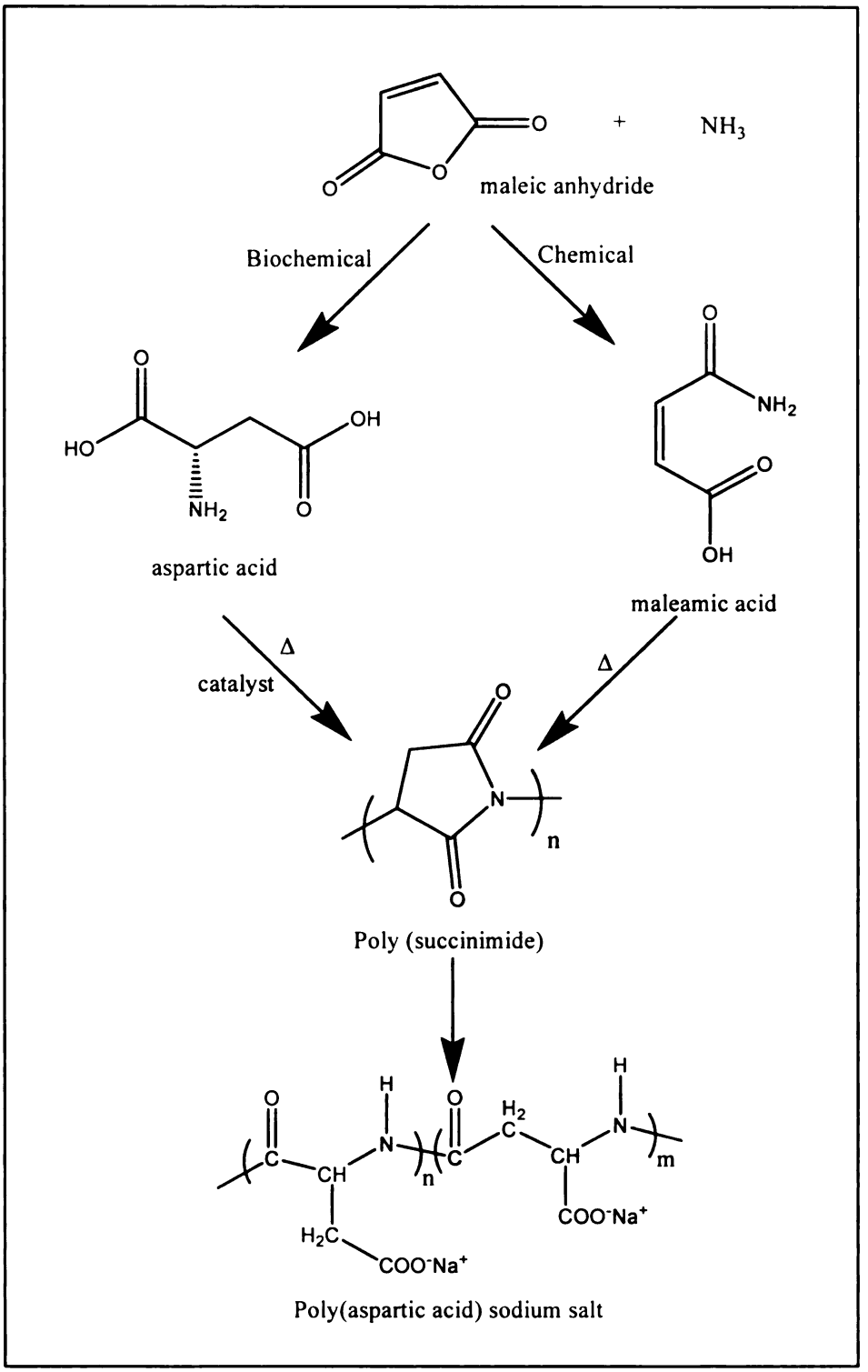

Figure 1.6 Synthetic routes explored to synthesize sodium polyaspartate. [25]

1.7 Choice of suitable polymers

For many years, the chemical industry has depended primarily on petroleum feedstock as a raw material. Now there are numerous indications that this approach is changing. Several companies are exploring biochemical routes for production of major chemicals and chemical intermediates. Examples include lactic acid (Cargill-Dow, Inc.), citric acid (Archer Daniels-Midland and Cargill Inc.), and 1,3 propanediol (Dupont). Other chemical intermediates that can be produced by fermentation and would have substantial market if production costs could be reduced by attainment of economy of scale. Succinic acid is one such example, which along with its derivatives has the potential of a multi-billion dollar chemical business.

1.7.1 Succinic acid: New platform for chemicals from renewable raw material

The fermentation technology developed by the Applied Carbochemicals, Inc. (ACC), under a Cooperative Research and Development Agreement (CRADA) with four US Department of Energy (DOE) laboratories, has a manufacturing cost for succinic acid that opens the possibility for its use in a number of applications. The resulting low cost succinic acid can potentially be converted into several industrially important chemicals. Figure 1.7 describes how succinic acid and its products could be used in numerous industrial applications. The emphasis of the current dissertation (shaded region in figure 1.7) is on the development and optimization of novel catalyst technology for the production of polymers from a simple monomer that could be synthesized in one or two steps from the succinic acid salts produced by the fermentation of sugars from agricultural sources. These polymers could then be used for novel applications as well as

to replace existing polymers. This dissertation focuses on the use of maleimide polymers as anti-scaling agents and as additives to alter polymorph ratio in calcium carbonate crystallization.

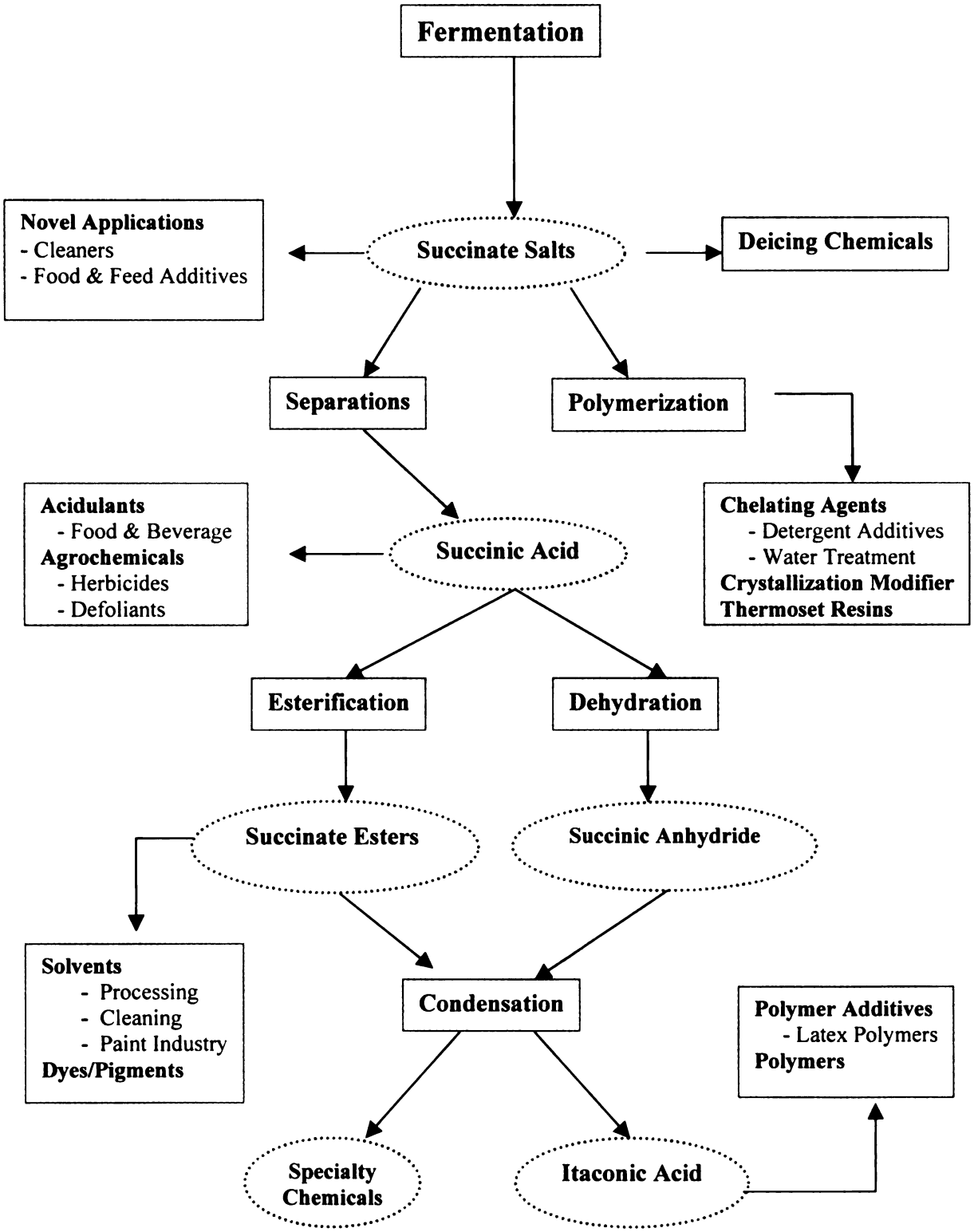

Figure 1.7 Possible synthetic routes and applications for various chemicals from succinic acid.

1.7.2 Maleimide as a monomer

Monomers that can be easily produced from succinic acid and succinate salts include succinic anhydride, succinimide, maleic anhydride, maleic acid, maleimide and N-substituted maleimide as shown in Figure 1.8. Succinic anhydride and succinimide lack a double bond for addition polymerization and their tendency to polymerize by ring opening is very poor. Maleic acid is not known to homopolymerize. Maleic anhydride has very low tendency to polymerize due to steric hindrance and high chain transfer constant to the monomer & initiator.[26] Maleimide, on the other hand, exhibits ease of polymerization compared to maleic anhydride and other nitrogen substituted maleimides. This feature is primarily due to formation of enol form of the propagating radical and the increased interaction of the enolized radical with monomer through hydrogen bonding. This also rules out the possibility of repulsion between growing chain and incoming monomer.

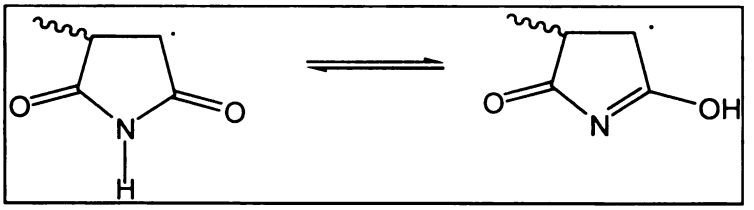

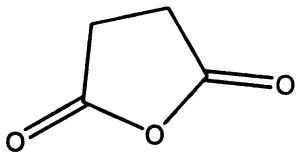

succinic anhydride

- Absence of C=C bond
- Low polymerization rate

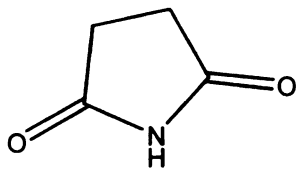

succinimide

- Absence of C=C bond
- Cyclic amide stable to ring opening

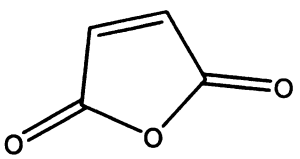

maleic anhydride

- Steric hindrance
- High chain transfer coefficient

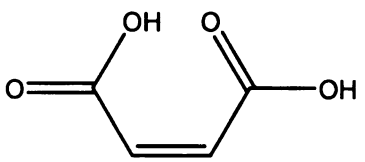

maleic acid

- Doesn't homopolymerize

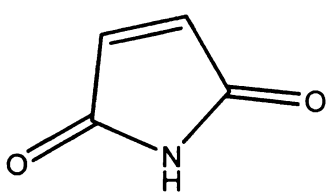

maleimide

- Higher rate of polymerization due to keto-enol tautomerism

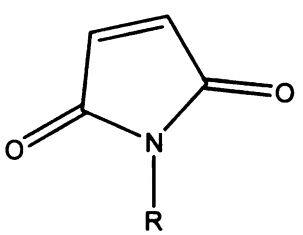

N substituted maleimides

- Steric hindrance

Figure 1.8 Potential succinic acid derived monomers for polymerization studies.

1.7.3 Polymerization of maleimide

Maleimide undergoes radical[27] as well as anionic polymerization.[28] Isomerization of the anion by proton transfer in anionic polymerization of maleimide leads to the formation of N-substituted isomerized units.

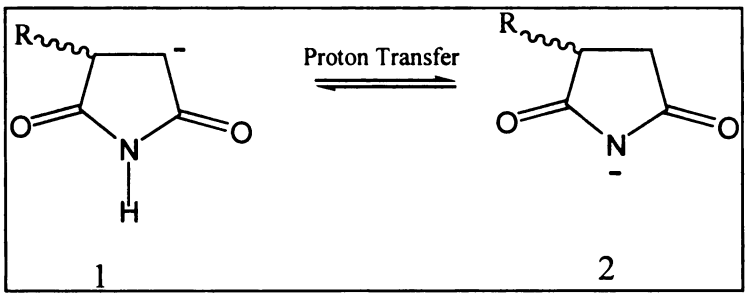

Therefore anion 1 either propagates to give C-C linked polymerized units or it can undergo isomerization to give anion 2, which forms N-substituted isomerized units in the polymer backbone. There is similar stabilization in the case of radical initiated polymerization to form resonance stabilized a succinimidyl radical (3, 4) by intramolecular tautomerization, but this radical is unable to propagate further and its formation is a monomolecular chain termination reaction.[29]

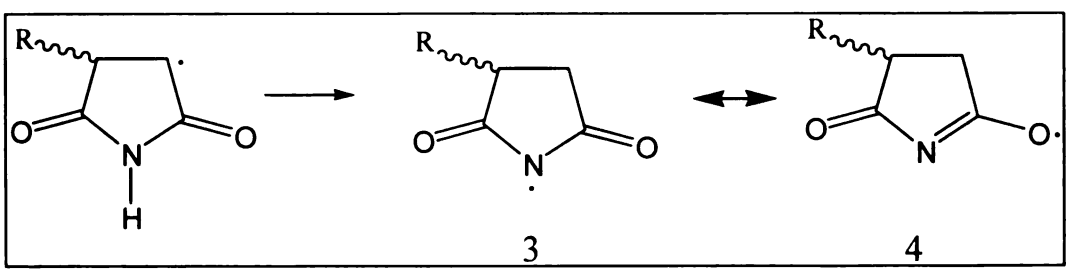

The anionic polymerization of the maleimide results in a mixture of C-C linked and C-N linked polymer chains.

Researchers have also used a variety of metal compounds in combination with alcohol initiator. These initiator systems, such as SnO, PbO and Pb(2-ethylhexanoate)$_2$, in combination with t-butyl benzyl alcohol, have been employed in maleimide polymerization.[30] These initiators have been reported for other systems, the most commonly cited is polymerization of lactide and substituted lactides. The polymerization has been shown to be a type of coordination polymerization resulting in high yield and molecular weight. The alcohols are vital for the action of the catalyst system since they coordinate with the metal compound to initiate the polymerization.

1.8 References

[1] Mullin, J. W.; Söhnel, O. *Chemical Engineering Science*, **1977**, 32, 683-686.

[2] Garside, J. *Chemical Engineering Science*, **1985**, 40, 3-26.

[3] Söhnel, O.; Mullin, J. W. *Chemical Engineering Science*, **1978**, 33, 1535-1538.

[4] Leeuwen, Van C. *Journal of Crystal Growth*, **1979**, 46, 91-95.

[5] Myerson, A.S. and Ginde, R. *Handbook of Industrial Crystallization,* Edited by Myerson, A. S., Butterworth-Heinemann, Boston, **1993**.

[6] Wankat, P. C. *Rate Controlled Separations*, Elsevier Science Publisher, London, **1990**, chapter 3, 4.

[7] Baird, J. K.; Hill, S. C.; Clunie, J. C. *Journal of Crystal Growth*, **1999**, 196, 220.

[8] http://www.nssga.org/whoweare/calcarbro.html.

[9] Koutsoukos, P. G.;Kontoyannis, C. G. *Journal of Crystal Growth,* **1984,** 69, 367-376.

[10] Tsuno, H. O.; Hiroyuki, K; Akaji, T. *Journal of Conf. Abtracts*, **2000**, 5, 2, 1022-1023.

[11] http://www.ibase093.eunet.be/en/ccawhat.html.

[12] Cothup, N. B; Daly, L. H.; Wiberly, S. E. *Introduction to Infrared and Raman Spectroscopy, 3rd edition,* Academic Press, Boston, **1990**.

[13] Pelletier, M. J. *Analytical Applications of Raman Spectroscopy,* Blackwell Science Ltd., Oxford, **1999**.

[14] Ingle, J. D. Jr.; Crouch, S. R. *Spectrochemical Analysis*, Prentice Hall; N. J., **1988.**

[15] Kaiser Optical Systems Inc., *Hololabseries 5000 Operations Manual*, Kaiser Optical Systems Inc., Ann Arbor MI, **1997**.

[16] Kontoyannis, C. G.; Orkoula, M. G.; Koutoukos, P. G., *Analyst*, **1997**, 122, 33-38.

[17] Kontoyannis, C. G.; Vagenas, N. V., *Analyst*, **2000**, 125, 251-255.

[18] Garside, J.; Tavare, N. S. *Chemical Engineering Science,* **1981**, 40, 1485.

[19] Wulff, G.; Z. Kristallogr., **1901**, 34, 449.

[20] Hartman, P.; Perdok, W. G. *Acta Cryst.*, **1955**, 8, 525-529.

[21] Elwell, D.; Scheel, H. J. *Crystal Growth from High Temperature Solution*; Academic Press, London, NY, **1975**.

[22] Mullin, J. W. *Crystallization*, 3rd Edition, Butterworth- Heinemann Ltd, Oxford, London, **1993**.

[23] Gerbaud, V.; Pignol, D.; Loret, E.; Bertrand, J. A.; Berland, Y.; Camps, F. C. J.; Canselier, P. J.; Gabas, N.; Verdier, M. J. *Journal of Biological Chemistry,* **2000**, 275, 2, 1057-1064.

[24] Burrill, K.A. *Journal of Crystal Growth*, **1972**, 12, 239.

[25] Freeman, M. B.; Paik, Y. H.; Swift, G.; Wilczynski, R.; Wolk, S. K.; Yocum, K. M. *ACS Symposium Series 626, American Chemical Society: Washington, DC*, **1996**, 118-136.

[26] Joshi, R. M. *Makromol. Chem.*, **1962**, 53, 33.

[27] Guang Q. C.; Zhi-Qiang W.; Jian-Ru W.; Zi-Chen L.; Fu-Mian L. *Macromolecules*, **2000**, 33, 232-234.

[28] Howard C. Haas, Ruby L. Macdonald, Journal of Polymer Science: Polymer Chemistry Edition, **1973**, 11, 327-343.

[29] Nakayama, Y.; Smets, G. *Journal of Polymer Science: Part A-1*, **1967**, 5, 1619-1633.

[30] Mao Y., Gregory, G. L., *Macromolecules*, **1999**, 32, 7711-7718.

Chapter 2

SYNTHESIS AND CHARACTERIZATION OF POLYMALEIMIDE BY BULK AND ANIONIC POLYMERIZATION TECHNIQUES *

Industrial & Engineering Chemistry Research, submitted August 2002.

Simplified syntheses of polymaleimide employing anionic polymerization (from the melt and from solution) and metal compounds-alcohol initiators such as PbO, SnO, Sn(2-ethyl hexanoate)$_2$ in presence of t-butyl benzyl alcohol are presented. The resulting polymers contain a combination of C-N and C-C connected monomers. Preliminary structures of the polymers were determined using NMR. The ratio of C-N and C-C connected monomers was determined and the percentage of C-N connected monomer units varied from 40 to 80 % with the higher percentage from anionic polymerization. The molecular weight of the polymers, as determined by gel permeation chromatography (GPC) with aqueous mobile phase and sodium polyacrylate standards, ranges between 1100 to 4200 for anionic polymerization and is about 11500 for metal oxide-alcohol initiated polymerization. Solution phase properties of the polymaleimides were evaluated by calcium chelation and precipitation inhibition studies.

2.1 Introduction

Water-soluble polymers are widely used as builders and anti-redeposition agents in the detergent industry. Polycarboxylate compounds, particularly polyacrylates and copolymers, are commonly used as dispersants and antiscalants in water-treatment and detergents.[1] Such polymers are used in low-phosphate or phosphate-free detergents to

minimize eutrophication of lakes and rivers caused by high concentrations of phosphorous compounds.

Several hundred million pounds of synthetic polymers are consumed annually as chelating agents and detergent builders. These compounds are usually released into the environment after use and the environmental impact is particularly important for the compounds that are not decomposed by natural processes (biodegradation).[1] Therefore, finding appropriate biodegradable polymers such as polyaspartic acid has been the motivation of several studies.

Biodegradability, excellent calcium chelation and antiscaling properties make sodium polyaspartate (SPA) a potential replacement for polyacrylic acid. SPA is commonly synthesized by hydrolysis of polysuccinimide with sodium hydroxide solution, and is a mixture of two isomers, α and β subunits, as shown in Figure 2.1. The structures of SPA and the ratio of the two isomers have been determined by ^{1}H NMR spectroscopy.[2,3]

Previously studied schemes for polysuccinimide synthesis employ aspartic acid, maleic acid, fumaric acid, maleamic acid, or the ammonium salt of maleic acid as the starting monomer.[4,5,6] The only efforts reported in literature for using maleimide as the starting monomer for polysuccnimide preparation is the one outlined in the Japanese patent (No 44-09394B). A base catalyzed approach, using maleimide as the monomer in the presence of a vinyl polymerization inhibitor was reported. However, this method was not explored further due to reasons that are unclear.

We report herein new approaches to base catalyzed polymerization for the preparation of polysuccinimide (alternatively called polymaleimide) using maleimide as the monomer. The product was characterized with ^{1}H, ^{13}C NMR, and ^{1}H/^{1}H NMR. Gel permeation

chromatography (GPC) was used to determine the molecular weight with reference to polyacrylate standards. The effect on solution calcium ion concentration was determined to evaluate the suitability of these synthesized polymers as detergent builders and chelators.

2.2 Experimental section

Unless otherwise specified, ACS reagent grade starting materials and solvents were used as received from commercial suppliers without further purification. Proton nuclear resonance (^{1}H NMR) analyses were carried out at room temperature on a Varian Gemini-300 spectrometer with solvent proton signals being used as chemical shift standards. Gel permeation chromatography (GPC) was performed with a Biorad HPLC system equipped with ultraviolet and refractive index detectors. A Supelco (GMPWXL, 7.8 mm × 30 cm, particle size of 13 μm) column was used for the GPC studies. The mobile phase used was 0.05M sodium sulfate in HPLC water and the flow rate was 0.6 mL/min. Temperature was maintained at 30 °C. The calibration curve for the GPC measurements was determined using polyaspartic acid standards with low molecular weight distribution. Potentiometric measurements were conducted with a calcium selective electrode purchased from Orion Research, Inc. (model 97-20 ionplus electrode). Maleimide was purchased from TCI America and was recrystallized two times from ethyl acetate before use.

2.2.1 Melt polymerization of maleimide

Maleimide was melt polymerized using metal compounds including PbO, SnO, and Sn(2-ethyl hexanoate)$_2$ in combination with t-butyl benzyl alcohol as initiators. Solvent-free polymerizations were carried out in sealed 3/8 inch diameter glass tubing. In a representative polymerization, 0.5 g of maleimide was placed in the glass tube and the appropriate amount of initiator was added. The contents were subjected to three cycles of freeze-pump-thaw. The glass tube was heat sealed while the vacuum was maintained. The sealed tube was immersed in a preheated oil bath maintained at 180 °C. At the end of the polymerization, the tube was cooled and opened, and the polymer was precipitated in either ethyl acetate or methanol. A portion of the sample was evacuated to dryness and analyzed by NMR for conversion. For hydrolysis of the polymer, a portion of the polymer was dissolved in water (10- 12 weight %) and a mole equivalent amount of sodium hydroxide was added. The polymer was hydrolyzed at 85 °C for 10-12 hours and lyophilized. The resulting polymer was dissolved in water (10-12 weight %) and precipitated in ethanol for purification. NMR, calcium-chelation, and GPC studies were performed on the polymer.

2.2.2 Anionic polymerization of maleimide [7-14]

Twenty grams of maleimide were placed in a beaker in an ice water-bath. A solution of KOH (2.5 g) in 2 mL of distilled water was added. The resultant slurry was stirred continuously with a glass rod. The color of the slurry changed from white to yellow, then to red. The reaction was completed in less than a minute. The beaker was removed from the ice water-bath and the contents were heated on a hot plate at about 80 °C to dryness.

The procedure for hydrolysis was the same as reported for the case of melt polymerization.

2.2.3 Anionic polymerization of maleimide in ethanol

Five grams of maleimide were dissolved in 25 mL of ethanol at 70°C (the temperature was controlled by an oil-bath) in a 100 mL round bottom flask. KOH solution (0.35 g in 10 mL ethanol) was added to the round bottom flask and the contents were maintained at 70°C for 2 hours. The color of solution changed from colorless solution to red followed by formation of pink precipitate. The pink solid was filtered immediately and dried in an oven around 80°C.

2.2.4 Chelation studies of polymers with calcium selective electrode

A series of calcium standard solutions (10-100 ppm as $CaCO_3$) were prepared to construct the calibration curve needed to determine the free calcium solution concentration in the presence of the polymers.[15] A stock solution of 0.01 M $CaCl_2$ (1000 ppm, hardness as $CaCO_3$) was prepared by dissolving 0.1109 g of $CaCl_2$ in 100 mL of water and then diluted to give the desired concentration. One-half gram of the hydrolyzed polymer was dissolved in 25 mL water for a stock solution of polymer. The electrode was immersed in 50 mL of a 200 ppm calcium solution at 25 °C and the solution was stirred continuously using a magnetic stirrer. The polymer solution was added in small increments (0.5 mL) of the stock solution, using Brinkmann® auto-titrator and the equilibrium value of free calcium ions present was noted after the reading stabilized. Titration was stopped when the potential value was lower than for 10 ppm calcium

solution. The data were normalized with respect to the calibration curve to allow a comparison with the various polymers tested.

2.2.5 Calcium carbonate precipitation inhibition

This test evaluates the polymer as an inhibitor for calcium carbonate precipitation and has been described in U.S. patent No. 5,152,902.[16] A 70-mL aliquot of 0.015 M $CaCl_2$ solution was placed in a beaker and 0.5 mL of inhibitor (polymer solution, 100 ppm) was added. The contents of beaker were stirred during the addition of 10 mL of 0.01M sodium bicarbonate. The resulting solution was titrated against 0.1 M sodium hydroxide with constant stirring until the solution became turbid. The solution pH was measured before and 10 minutes after the addition of sodium hydroxide solution. The amount of sodium hydroxide solution consumed in each titration was recorded.

2.3 Results and Discussion

2.3.1 Structure analysis

The polymerization of maleimide was very rapid under the conditions used in the current studies. Polymaleimide formed by the various techniques possessed both C-N and C-C connected monomer units, as shown in Figure 2.1. These polymers were hydrolyzed to form the corresponding sodium salts. The C-N connected monomer gave α and β forms (Figure 2.1), depending on the bond that was hydrolyzed.

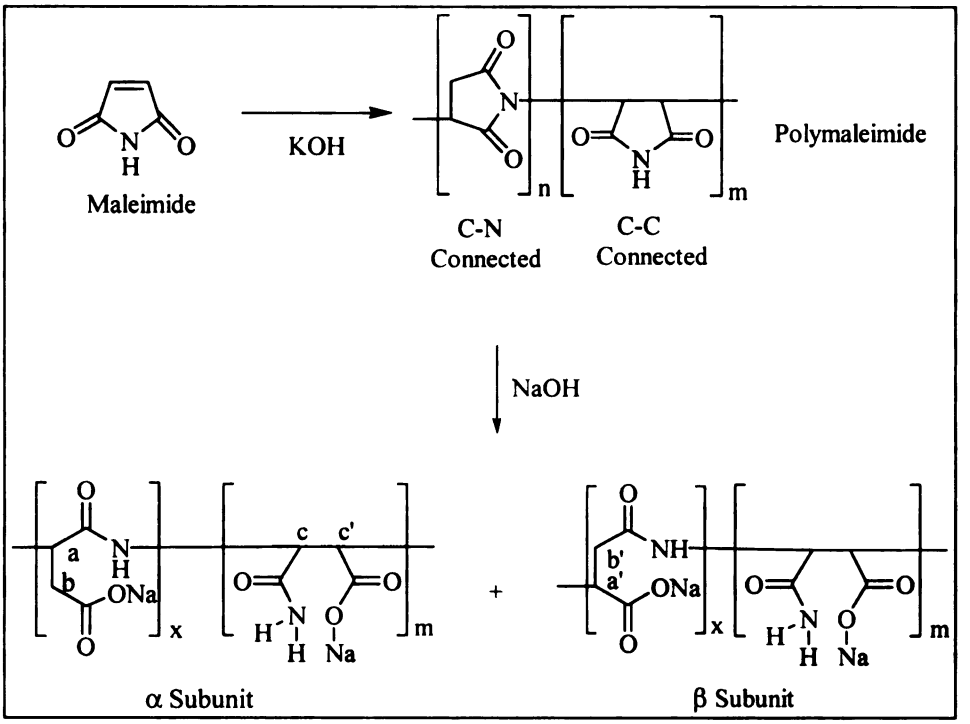

Figure 2.1 Synthesis and hydrolysis of maleimide.

A Distortionless Enhancement by Polarization Transfer (DEPT) spectrum of polymaleimide synthesized by anionic, solvent free polymerization is shown in Figure 2.2. The CH_2 peak at 34 ppm and CH peak at 51 ppm indicate that it contains C-N connected monomer since the CH carbon is attached to N and therefore quite deshielded. The CH peak at 36 ppm indicates that it also contains C-C connected monomers. These data confirm the existence of the structures further studied by ^{1}H NMR.

^{1}H NMR spectroscopy was used to determine the ratio of C-N and C-C bonds. Typical ^{1}H NMR spectra are shown in Figure 2.3. The peak at 4.25 ppm is of protons from C-N connected monomers (a and a'). The peak at 2.45 ppm is the combination of protons from C-N and C-C connected monomers (b, b', c, and c'). Therefore, the percent of C-N connected monomers could be easily figured out from integration of the two peaks[3] (see figure 2.4), which is 38.5 % in this case. The percent of C-N in case of anionic polymerization was determined in a similar way and was around 80%. Due to the overlap of the water peak, the ratio of α and β subunits cannot be calculated accurately. There are some small peaks between 5.5 to 6.5 ppm that correspond to end groups. The full set of results is presented in Table 2.1.

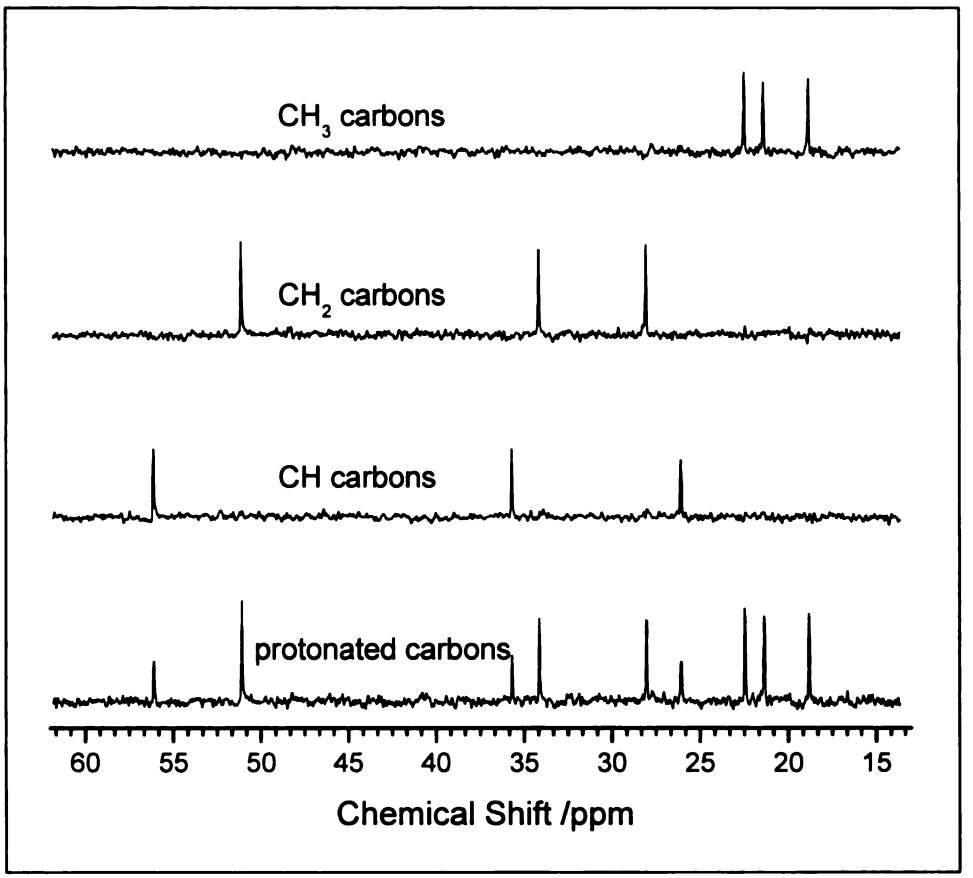

Figure 2.2 DEPT spectrum of polymaleimide made by KOH initiated anionic, solvent free polymerization.

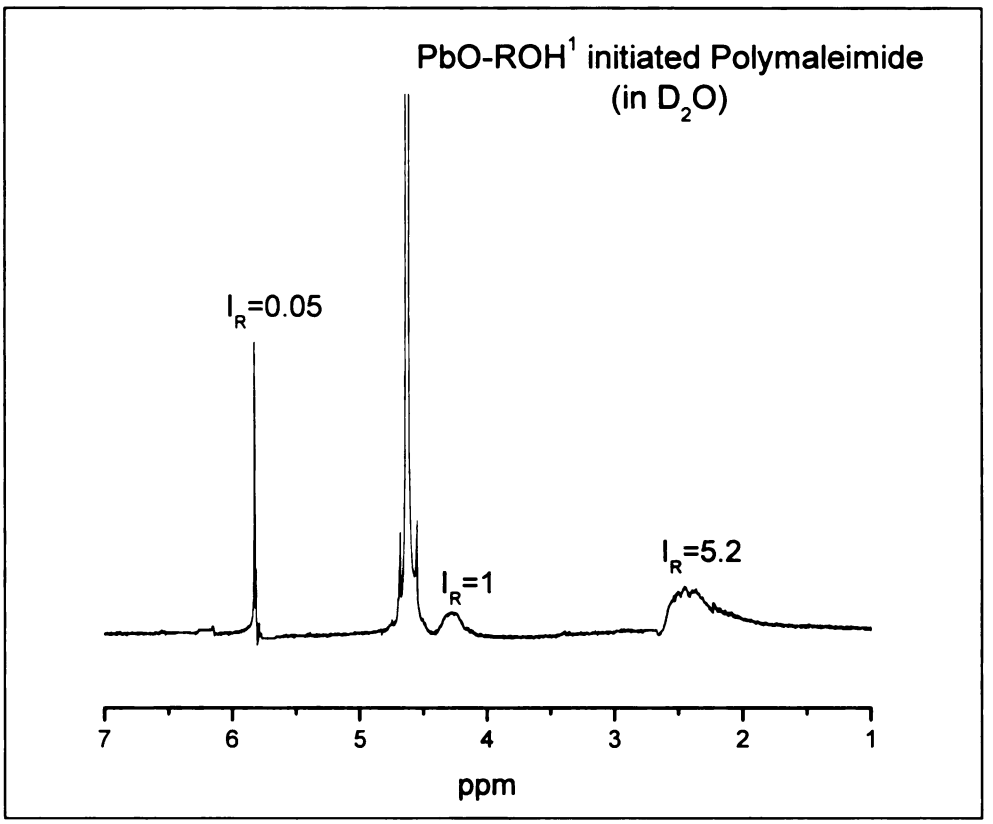

Figure 2.3 Proton NMR Spectrum of Polymaleimide made by bulk polymerization with PbO-ROH[1] initiator.

I_R is the peak intensity.

[1]ROH refers to t-butyl benzyl alcohol.

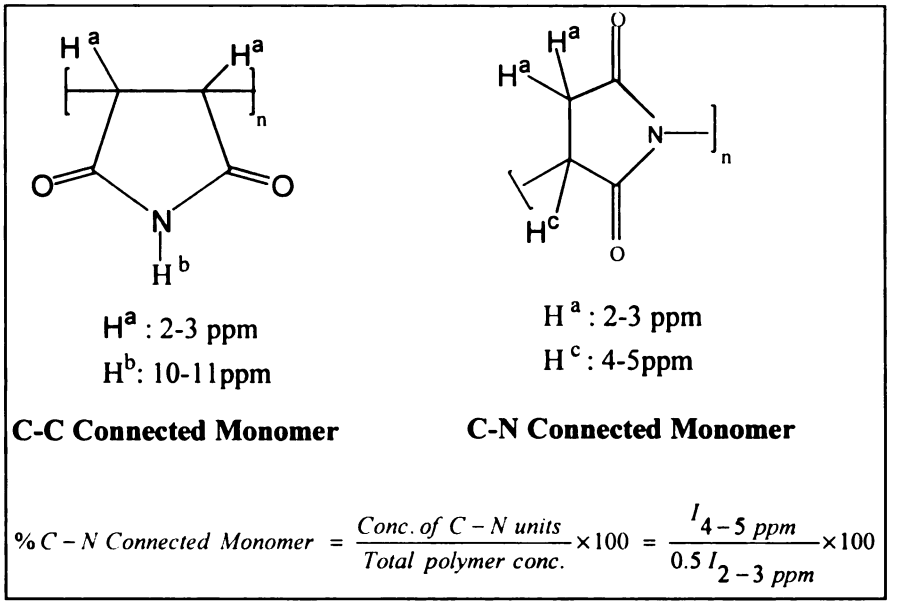

Figure 2.4 Calculation of percent C-N connected monomer by ^{1}H-NMR technique.

Gel Permeation Chromatography (GPC) was used for determining the molecular weight of polymers. Sodium salts of polyacrylic acid possess similar molecular structures as polymaleimides; therefore, they were used as standards for our studies. A calibration curve was generated with four standards and the molecular weights of the synthesized polymers were determined using this calibration. The weight average molecular weight, M_W, was determined to be around 11500 for bulk polymerization of maleimide using lead oxide-t-butyl benzyl alcohol initiator, 1100 for solid phase polymerization using KOH. Solution polymerization of maleimide in ethanol gave polymers with M_W around 4200. The full results are presented in Table 2.1.

2.3.2 Application studies

2.3.2.1 Calcium carbonate precipitation inhibition

The activity of polymaleimide polymers as inhibitors for calcium carbonate precipitation was studied with respect to Acusol®, a commercial detergent builder. The ability of polymers to act as inhibitor was evaluated by the consumption of NaOH, and pH drop.[16] Higher amount of NaOH consumed and smaller pH drop correspond to a better inhibitor. The experimental results are listed in Table 2.2. PbO-t-butyl benzyl alcohol initiated PMI required maximum amount of sodium hydroxide and had minimum pH drop; therefore, would be expected to perform better than the other polymers that were studied.

Polymer	Percent Conversion [1]	C-N Connected Monomer (%) [1]	Molecular Weight [2]
PMI_Cu(tpp)$_2$NO$_3$-ROH [3]	95.6 ± 0.5	43.2 ± 0.8	5900 ± 100
PMI_KOH initiated	92.8 ± 0.3	79.8 ± 0.9	1100 ± 180
PMI_PbO_ROH [3]	99.0 ± 0.5	38.7 ± 0.8	11500 ± 90
PMI_KOH_ethanol [4]	44.2 ± 0.2	77.2 ± 0.6	4200 ± 150
PMI_SnO-ROH [3,4]	21.7 ± 0.4	36.7 ± 0.6	10800 ± 80
PMI_Sn(2-ethyl hexanoate)$_2$- ROH [3,4]	25.3 ± 0.7	38.3 ± 0.7	11200 ± 120

Table 2.1 Properties of the polymers synthesized by different methods.

[1] by ratio of peak integration (mean of three different runs).

[2] M_n by GPC with respect to polyacrylate standards (mean of three different runs).

[3] ROH refers to t-butyl benzyl alcohol.

[4] Not used for further studies due to low conversion.

Inhibitor	NaOH sol. used (mL)[1]	ΔpH^2 $xx \pm \sigma$
PMI_Cu_sys[3]	2.300 ± 0.005	0.75 ± 0.05
Acusol®	2.470 ± 0.005	0.95 ± 0.05
PMI_KOH[4]	2.475 ± 0.005	1.04 ± 0.05
PAA[5]	2.755± 0.005	0.70± 0.05
PMI_PbO[6]	2.925 ± 0.01	0.65 ± 0.07

Table 2.2 Comparison of chelating behavior of polymers.

[1] [NaOH] = 0.1 M.

[2] Mean of five measurements ± Standard deviation.

[3] *PMI_Cu_sys* refers to Polymaleimide synthesized by bis(triphenylphosphine) Cu(I) nitrate and t-butyl benzyl alcohol initiator.

[4] *PMI_KOH* refers to Polymaleimide synthesized by KOH initiator.

[5] *PAA* refers to Polyacrylic acid.

[6] *PMI_PbO* refers to Polymaleimide synthesized by PbO and t-butyl benzyl alcohol initiator

2.3.2.2 Calcium chelation studies

The performance of polymers as a detergent builder can also be judged by calcium chelation studies. The basis of this technique is that the calcium selective electrode measures only the free calcium ions and not the chelated (bound) calcium ions. The lower the concentrations of free calcium ions, the stronger the calcium chelation. A calibration curve of voltage versus calcium concentration was generated with several standard Ca^{2+} solutions, which resulted in a linear plot over the range of interest. The concentration of free calcium ions after addition of a known amount of inhibitor polymer solution was determined from this calibration curve. The curves for different polymer solutions are shown in Figure 2.5. Clearly, PMI prepared by PbO-t-butyl benzyl alcohol initiator and by anionic polymerization using KOH shows the best chelation with calcium and their chelating properties are comparable to commercial polyaspartic acid. Therefore, they would be the most efficient anti-scaling agent. These results are consistent with the results of the calcium carbonate precipitation inhibition studies described earlier.

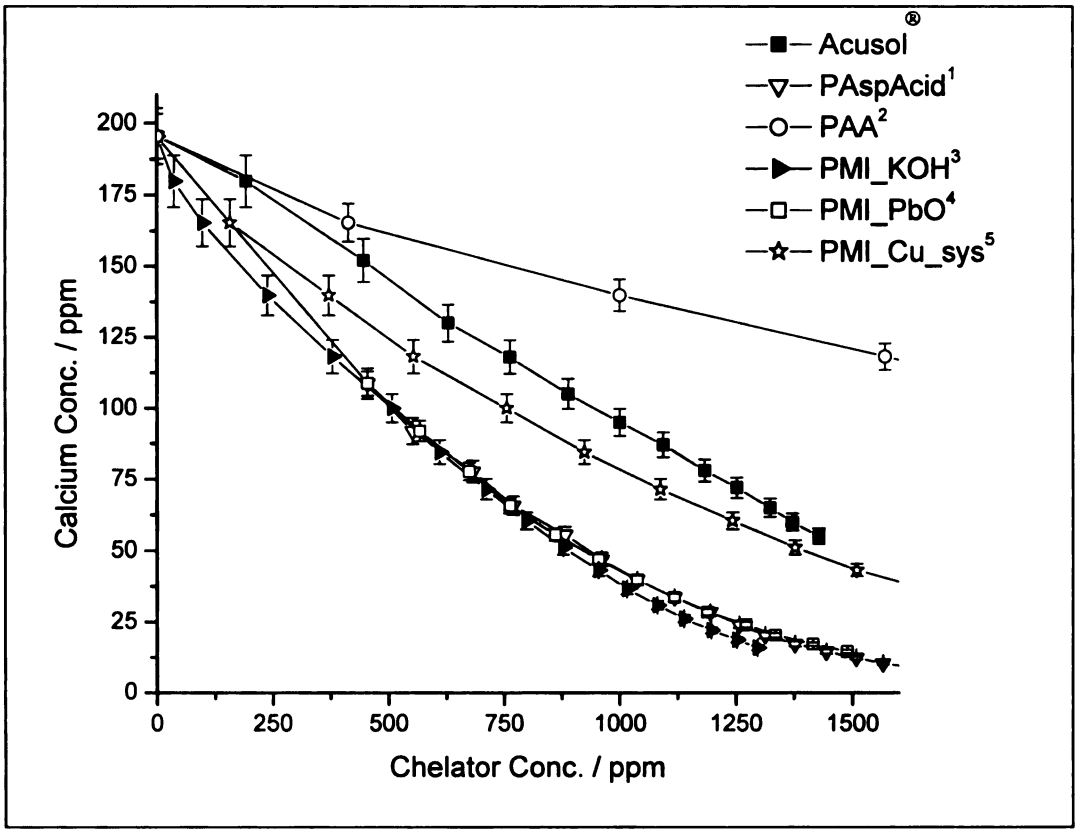

Figure 2.5 Chelation studies of polymers to determine their effectiveness as anti-scaling agent using calcium selective electrode.

Error bars represent ±σ, N = 3.

[1]*PAspAcid* refers to Polyaspartic acid.
[2]*PAA* refers to Polyacrylic acid.
[3]*PMI_KOH* refers to Polymaleimide synthesized by KOH initiator.
[4]*PMI_PbO* refers to Polymaleimide synthesized by PbO and t-butyl benzyl alcohol initiator.
[5]*PMI_Cu_sys* refers to Polymaleimide synthesized by bis(triphenylphosphine) Cu(I) nitrate and t-butyl benzyl alcohol initiator.

2.4 Conclusions

The differences in the properties of PMI synthesized under varying conditions are due to the variations in their molecular weight and the percentage of C-N connected polymers. Since melt polymerization using a metal oxide-alcohol initiator results in better properties of the polymer with respect to calcium binding, the C-C connected monomers apparently provide more accessible binding sites. The higher molecular weight polymers appear to have improved chelating properties; however, the effect of molecular weight requires a more thorough study than that reported here. In summary, simple methods for synthesis of polymaleimide from a maleimide monomer were employed and the resulting polymers compare favorably to existing commercial polyacrylates used in detergent formulation.

2.5 Acknowledgments

The author wishes to thank Applied CarboChemicals, Inc. and the Center for New Plant Products and Processes at Michigan State University for financial support of this work.

2.6 References

[1] Freeman, M. B.; Paik, Y. H.; Swift, G.; Wilczynski, R.; Wolk, S. K.; Yocum, K. M. *ACS Symposium Series 626, American Chemical Society: Washington, DC*, **1996**, pp. 118-136.

[2] Matsubara, K.; Nakato, T.; Tomida, M. *Macromolecules* **1997**, *30*, 2305-2312.

[3] Wolk, S. K.; Swift, G.; Paik, Y. H.; Yocom, K. M.; Smith, R. L.; Simon, E. S. *Macromolecules* **1994**, *27*, 7613-7620.

[4] Freeman, M. B.; Paik, Y. H.; Simon, E. S.; Swift, G. *U.S. Patent 5,393,868*, **1995**.

[5] Mosig, J.; Gooding, C. H.; Wheeler, A. P. *Ind. Eng. Chem. Res.* **1997**, *36*, 2163-2170.

[6] Sikes, C. S. *U.S. Patent No.5,981,691*, **1999**.

[7] Kojima, K.; Yoda, N.; Marvel, C. S. *J. Polym. Sci. Polym. A-1*, **1966**, *1*, 1121-1131.

[8] Tawney, P. O.; Snyder, R. H.; Conger, R. P.; Leibbrand, K. A.; Stiteler, C. H.; Williams, A. R. *J. Org. Chem.* **1961**, *26*, 15-21.

[9] Bamford, C. H.; Burley; J. W. *Polymers*, **1973**, 14, 395

[10] Haas, H. C.; Macdonald, R. L. *J. Polym. Sci. Polym. Chem. Ed.*, **1973**, *11*, 327-343.

[11] Haas, H. C. *J. Polym. Sci. Polym. Chem. Ed.*, **1973**, *11*, 315-318.

[12] Haas, H. C.; Moreau, R. D. *J. Polym. Sci. Polym. Chem. Ed.*, **1975**, *13*, 2327-2334.

[13] Decker, D. *Die Makromolekulare Chemie*, **1973**, *168*, 51-58.

[14] Bamford, C. H.; Bingham, J. F.; Block, H. *Trans. Faraday Soc.* **1970**, *66*, 2612-2621.[15]

[15] Craggs, A.; Moody, G. J.; Thomas, J. D. *Analyst* **1979**, *104*, 961-972.

[16] Koskan, L. P.; Low, K. C.; Meah, A. R. Y.; Atencio, A. M. U.S. Patent, 5,152,902, **1992**.

Chapter 3

MONITORING OF CALCIUM CARBONATE CRYSTALLIZATION IN THE PRESENCE OF POLYMERIC ADDITIVES USING NEPHELOMETRY

Polyaspartic acid and its copolymers have been proposed as substitutes for polyacrylic acid in detergent industry. Polymers synthesized from maleimide and subsequently hydrolyzed yield structures similar to polyaspartic acid. The efficiency of these maleimide polymers with respect to calcium carbonate crystallization was studied using nephelometry. Induction time and percent growth inhibition was determined for each polymeric additive. Polymaleimide synthesized by KOH initiated polymerization exhibited the greatest growth inhibition and longest nucleation time among the polymers investigated.

3.1 Introduction

Turbiditmetry and nephelometry are methods that measure the concentration of particulate matter in a suspension. The progress of crystallization from solution is associated with changes in the number and size of suspended particles in solution.[1] Therefore, these techniques are appropriate for estimation of parameters associated with crystallization kinetics. Both techniques are based on elastic scattering of radiation from the suspended particles, but differ in light collection geometry. Turbidimetry utilizes the decrease in intensity of transmitted radiation due to particle scattering; while nephelometry relies on the radiant power of the scattered radiation itself. A schematic of the instrumentation for the two techniques[2] is shown in Figure 3.1.

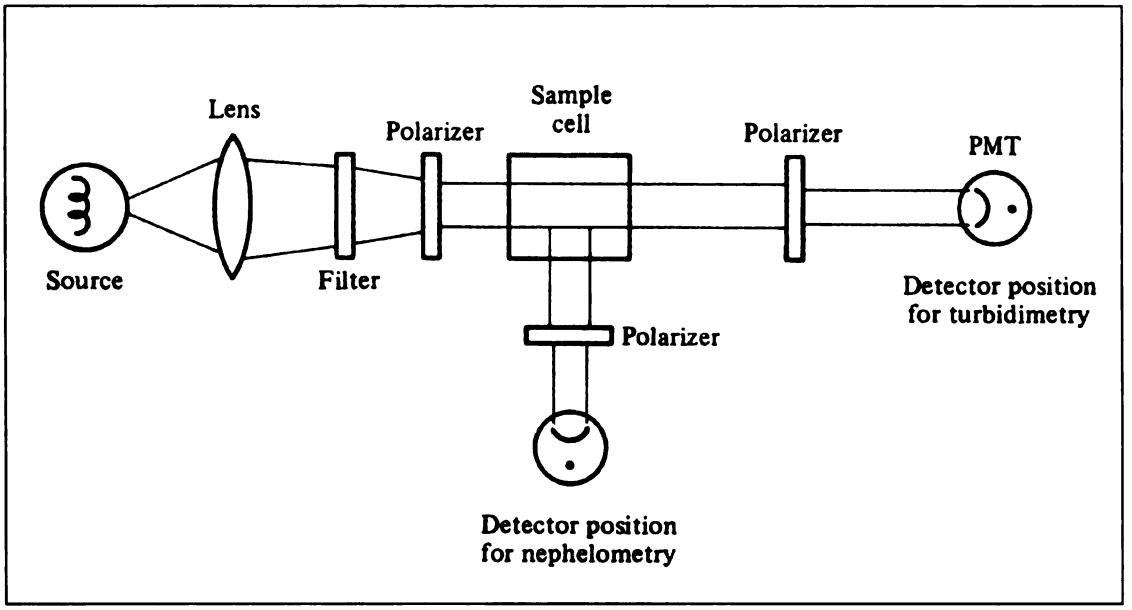

Figure 3.1 Instrumentation for turbidimetry and nephelometry.

* Detector is placed at right angle for nephelometry & in line for turbidimetry.

Adapted from *Spectrochemical Analysis* by James D. Ingle, Stanley R. Crouch.

Turbidimetry is preferred when the concentration of suspended particles is high. The high concentration of suspended particles results in a large change in the transmitted radiant power. Large amounts of scattering lead to more interferences and non-linearity in the case of nephelometry, reducing its accuracy at high particle concentrations.[3]

Nephelometry was chosen for the current studies because of relatively low concentration of suspended particles. In this case radiant power of scattering is small and nephelometry is preferred since changes in transmitted radiant power are not high enough for accuracy, especially during the initial phase of batch crystallization from particle free solutions. The scattering of radiation by suspended particles is called the Tyndall effect[4] and forms the basis of nephelometry. Nephelometry measurements are made in the ultraviolet and the visible region and therefore the size of the colloidal particles that can be measured are in the range of 100 nm to 700 nm in diameter.[5]

Crystal nucleation and its growth rate are two of the most important kinetic phenomena in crystallization from solution. The goal of the current study was qualitative determination and comparison of the effects of various polymaleimides on calcium carbonate crystallization. Evaluating the effect of additives on crystal growth rate was done by comparing the growth inhibition of calcium carbonate crystallization attained in presence of these polymers by comparison of the slopes of the nephelometry curves during the growth phase.[6] The effects of additives on nucleation were related to the induction time, which is the time lag between the supersaturation generation and its subsequent detection.[7]

3.2 Materials and Methods

ACS reagent grade starting materials and solvents were used as received from commercial suppliers without further purification, unless otherwise specified. The polymers used for the crystallization kinetics studies were synthesized by a number of techniques and using a variety of initiator systems. The initiator systems were KOH and various metal compound-alcohol combinations, while the polymerizations were carried out either in solution with water or ethanol as solvents, or by bulk solvent-less polymerization in the melt phase. Details of the synthesis of these polymers have been described in chapter 2. Table 3.1 provides a list of polymers used and their properties.

3.2.1 Nephelometry

A SPEX Fluorolog 1681 spectrofluorometer was used for the experiments and a schematic is shown in Figure 3.2. Light from the source (150 W xenon lamp) was focused on the sample after it passed through the excitation monochromator. The scattered light from the sample was reflected to the front-face collection port in the sample compartment and collected by an emission monochromator. The light was directed to a photomultiplier tube (PMT) for detection. The experiments were performed at 550 nm because this wavelength provided excellent signal to noise ratio and the xenon lamp output profile in this region has a flat baseline in frequency domain.

The instrument is designed for florescence measurements and for a one-cm path length cuvette as the sample cell, therefore, a slight modification was necessary for the current crystallization studies. A magnetic stir plate was placed under the sample compartment to assure mixing as the measurements were done in real time. Maintenance of sample homogeneity is critical for accurate and reproducible results, therefore, (as shown in

Figure 3.3) a special 40 mL cell was designed which had a quartz (uv transparent) bulb fused at the base of a one-cm path length cuvette to permit use of a magnetic stir bar. Experiments were performed in the 40 mL quartz cell and the supersaturation was generated at zero time by mixing stoichiometric amount of calcium and carbonate solutions to give a final concentration of 160 and 240 ppm of calcium and carbonate, respectively. Inhibitor solution, if any, was added after the addition of calcium solution, but prior to addition of carbonate. The solution was kept homogenous by stirring with a Teflon coated magnetic stirring bar. The total volume was kept constant at 39.5 mL by varying the amount of water added. After the supersaturation was generated, the intensity of scattered light was recorded every second using the PMT. The sample cell was washed with one molar hydrochloric acid solution between runs.

S.No.	Inhibitor	Source	Percent Conversion[1]	C-N Connected Monomer (%)[1]	Molecular Weight [2]
1	PMI_Cu_sys[3]	Synthesized	95.6 ± 0.5	43.2± 0.8	5900± 100
2	PMI_KOH[4]	Synthesized	92.8± 0.3	79.8± 0.9	1100± 180
3	PMI_PbO[5]	Synthesized	99.0± 0.5	38.7± 0.8	11500± 90
4	PAA[6]	Aldrich	-	-	5000
5	PaspAcid[7]	Bayer Corp.	-	-	-
6	Acusol®	Rhom & Haas	-	-	5000

Table 3.1 Properties of the polymers used as additives for nephelometry studies

[1] by ratio of peak integration (mean of three different runs)

[2] M_n by GPC with respect to polyacrylate standards (mean of three different runs)

[3] *PMI_Cu_sys* refers to Polymaleimide synthesized by bis(triphenylphosphine) Cu(I) nitrate and t-butyl benzyl alcohol initiator.

[4] *PMI_KOH* refers to Polymaleimide synthesized by KOH initiator.

[5] *PMI_PbO* refers to Polymaleimide synthesized by PbO and t-butyl benzyl alcohol initiator.

[6] *PAA* refers to Polyacrylic acid.

[7] *PaspAcid* refers to Polyaspartic acid.

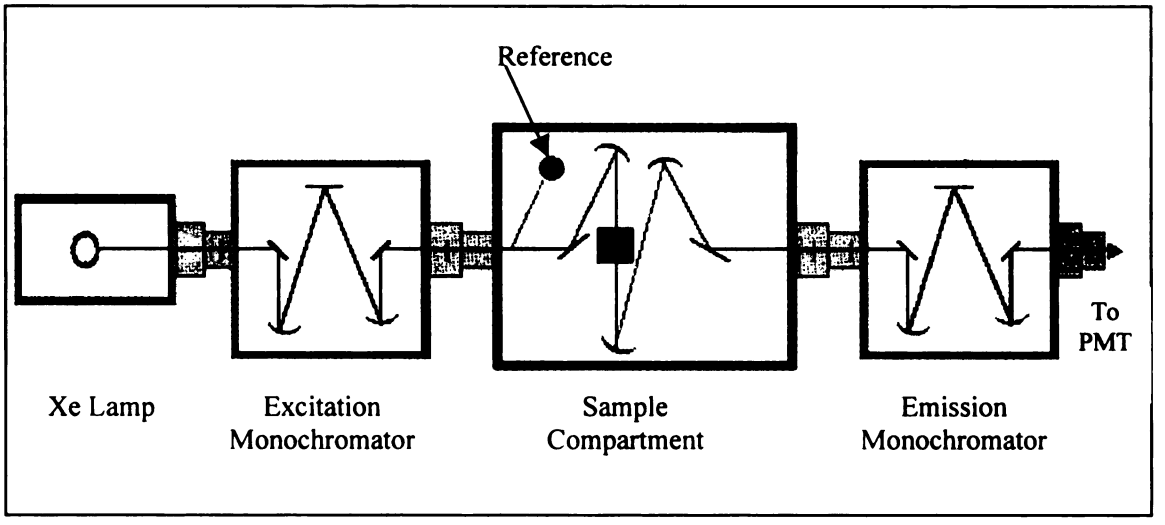

Figure 3.2 Optical Schematic of Flurolog-2 spectrometer used for nephelometry measurements.

Collection Mode : Nephelometry.
Software : DM 3000 from Spex Industries Inc.
Reference : Rhodamine-B.

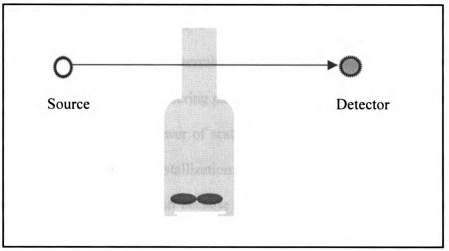

Figure 3.3 Experiment setup showing improvised cell used for nephelometry experiments.*

*Quartz bulb was fused to the base of a 1 cm path length cuvette.

3.3 Results

In nephelometry, the scattered radiant power Φ_{SC} is related empirically to the concentration of suspended particles by the following equation

$$\Phi_{SC} = \Phi_0 K_{SC} C$$

where K_{SC} is an experimentally determined constant,Φ_0 is the incident radiant power, and C is the concentration of the scattering particles. The size and shape of the particles have a large effect on the radiant power of scattering.[8] The number and size of particles is a function of time in batch crystallization; therefore, nephelometry is a good tool for kinetics studies of crystallization because it is sensitive to number (nucleation) and size (growth) of crystals.

Figure 3.4 shows a typical scattering curve obtained using nephelometry for the batch crystallization of calcium carbonate. Mixing the calcium and carbonate solutions created the supersaturation at zero time. Although the solution was supersaturated in region 1, no crystals were observed. Region 2 corresponds to a region dominated by self-nucleation therefore the signal intensity begins to rise. Crystal growth is dominant in region 3 and causes a decline in supersaturation. The solution returns to saturation in region 4 and there is no further crystallization. The induction time was determined by measuring the time at which the change in signal intensity was five percent of its maximum.[9,10] The induction times are related to the effect of additive on the crystal nucleation rate. The longer the induction time for crystallization, the greater is the inhibitory effect of the polymer additive on nucleation kinetics.[10]

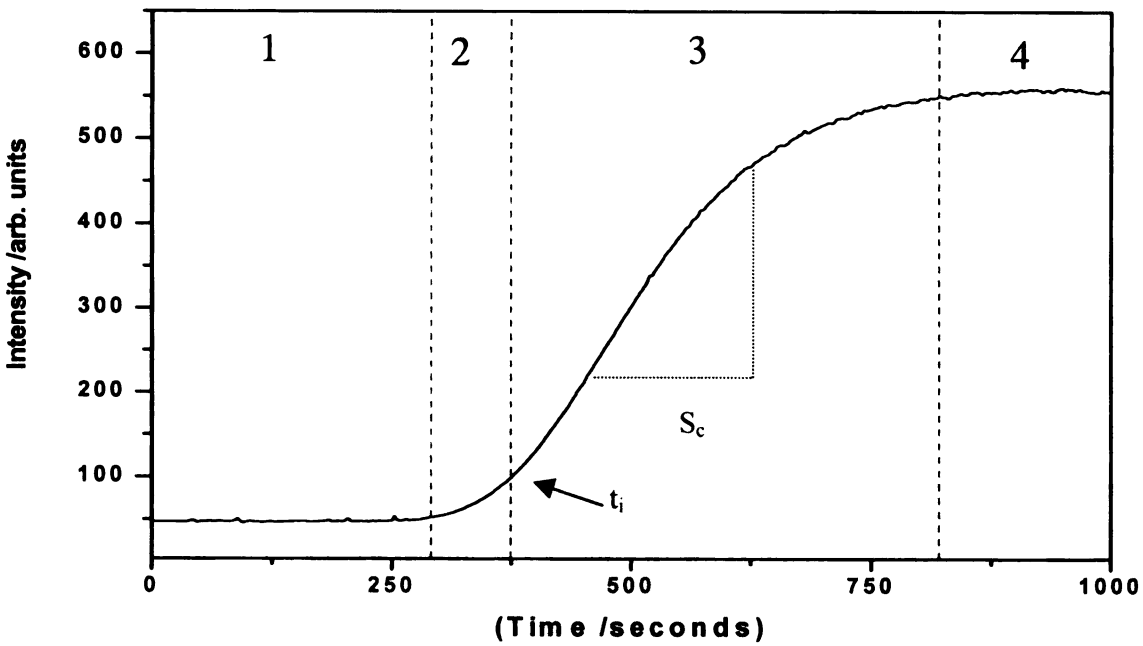

Figure 3.4 A typical nephelometry curve for calcium carbonate crystallization showing the four distinct regions during batch crystallization.

Region 1 Supersaturated solution, no crystals *Region 2* Self nucleation.

Region 3 Crystal growth and nucleation *Region 4* Saturated solution.

t_i represents the induction time for crystallization.

S_c represents the slope of region 3 and corresponds to crystal growth rate.

Growth inhibition was determined by calculating the slopes, S_c of the nephelometry curves in the absence and presence of inhibitor using the following formula.

$$\%\,Growth\;\;Inhibition\;\; = \frac{Slope^{\;Blank} - Slope^{\;Additive}}{Slope^{\;Blank}} \times 100$$

Blank is precipitating system without any additive

Inhibitor concentration was varied to observe the effect on induction time and percent growth inhibition. As shown in Figure 3.5 and 3.6, the polymaleimide additives have a varied effect on the crystallization kinetics of calcium carbonate. Polymaleimide synthesized by anionic polymerization using potassium hydroxide has the most pronounced effect on both induction time and percent growth inhibition followed by polyaspartic acid.

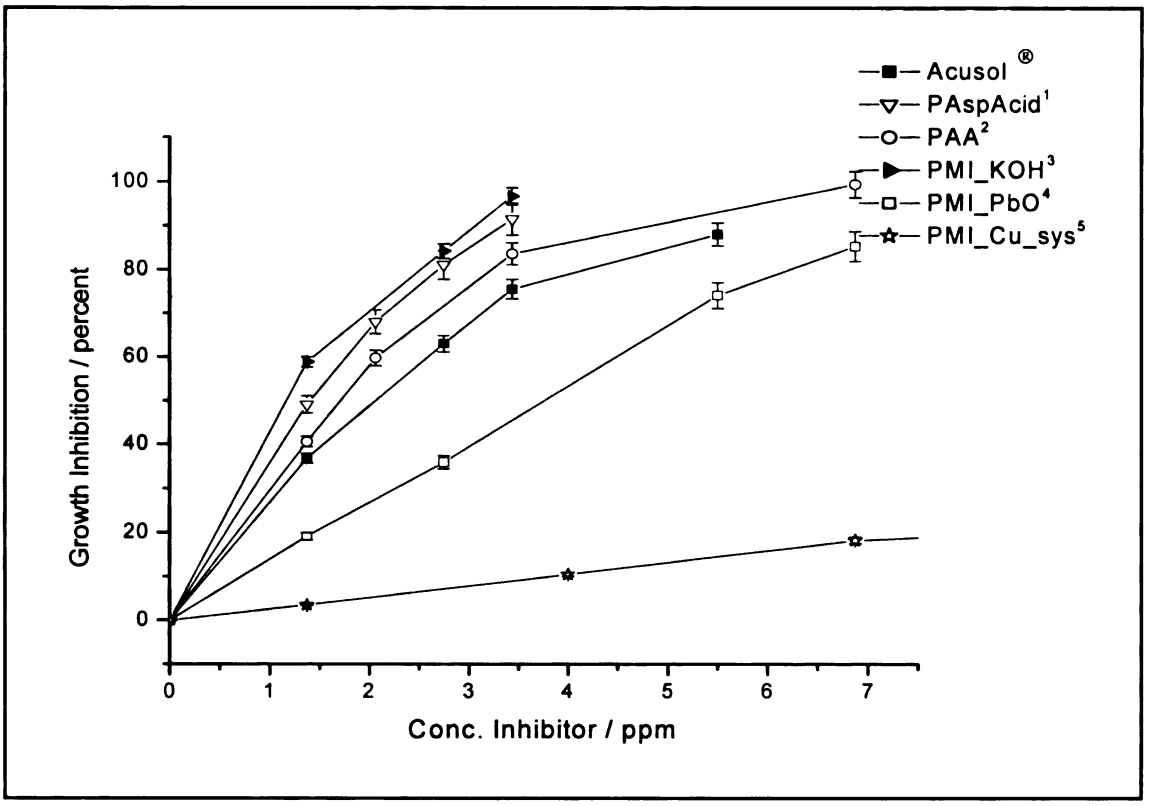

Figure 3.5 Comparison of synthesized polymers as growth inhibitors by measuring the change in slope of nephelometry curve of calcium carbonate crystallization in presence of various polymeric inhibitors.

Percent growth inhibition is defined as

$$\%Growth\ \ Inhibition\ = \frac{Slope^{\ Blank} - Slope^{\ Additive}}{Slope^{\ Blank}} \times 100$$

Error bars represent ±σ, N = 3.

Experimental conditions: Concentration of Ca^{2+} and CO_3^{2-} : 160 and 240 ppm, respectively.

Total volume : 39.5 mL.

Wavelength of light : 550 nm.

Collection mode : Nephelometry.

[1]*PAspAcid* refers to Polyaspartic acid.
[2]*PAA* refers to Polyacrylic acid.
[3]*PMI_KOH* refers to Polymaleimide synthesized by KOH initiator.
[4]*PMI_PbO* refers to Polymaleimide synthesized by PbO and t-butyl benzyl alcohol initiator.
[5]*PMI_Cu_sys* refers to Polymaleimide synthesized by bis(triphenylphosphine) Cu(I) nitrate and t-butyl benzyl alcohol initiator.

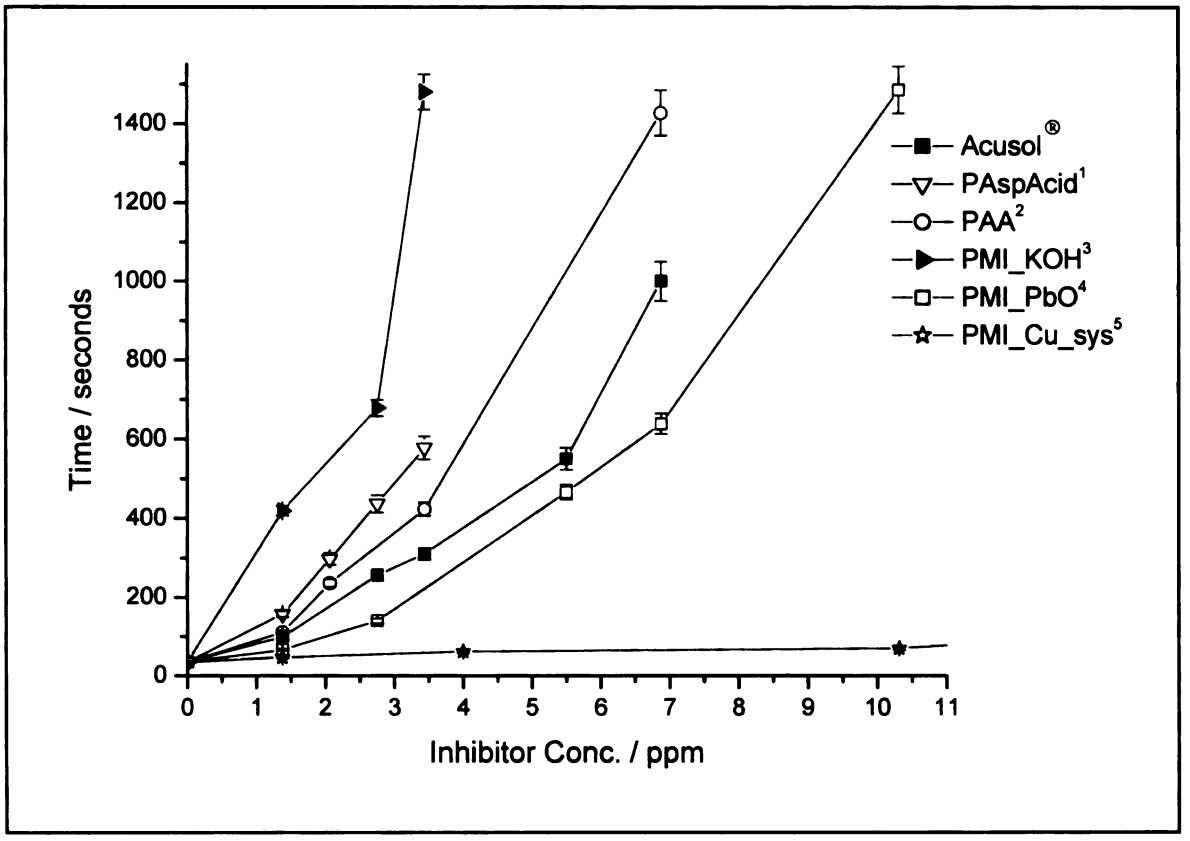

Figure 3.6 Comparison of synthesized polymers as growth inhibitors by measuring the increase in induction time of calcium carbonate crystallization in presence of various polymeric inhibitors.

Induction time is defined as time needed for signal intensity to be five percent of its maximum.

Error bars represent ±σ, N = 3.

Experimental conditions: Concentration of Ca^{2+} and CO_3^{2-} : 160 and 240 ppm, respectively.

Total volume	: 39.5 mL.
Wavelength of light	: 550 nm.
Collection mode	: Nephelometry.

[1] *PAspAcid* refers to Polyaspartic acid.
[2] *PAA* refers to Polyacrylic acid.
[3] *PMI_KOH* refers to Polymaleimide synthesized by KOH initiator.
[4] *PMI_PbO* refers to Polymaleimide synthesized by PbO and t-butyl benzyl alcohol initiator
[5] *PMI_Cu_sys* refers to Polymaleimide synthesized by bis(triphenylphosphine) Cu(I) nitrate and t-butyl benzyl alcohol initiator.

3.4 Conclusions

Nephelometry was employed as a fast, simple and reliable method for comparing the effect of various polymeric additives on crystallization of calcium carbonate. It gave information about both the important aspects of crystallization kinetics, namely crystal nucleation rate and growth rate. Induction time and percent growth inhibition determined are dependent on several experimental parameters such as wavelength of light used or method used for induction time calculation. However, the trends observed for induction time and percent growth inhibition would remain the same under any given set of experimental condition. The importance of this technique is therefore more with respect to comparison rather than determination of absolute parameters. Polymaleimide synthesized by anionic polymerization using potassium hydroxide as the initiator was the best additive for inhibiting both nucleation and growth rate of calcium carbonate crystallization. This was evident from its longest induction time and highest percent growth inhibition. This polymer is a good candidate for potential further study in anti-scaling and anti-redeposition applications.

3.5 Acknowledgment

The author wishes to thank Applied CarboChemicals, Inc. and the Center for New Plant Products and Processes at Michigan State University for financial support of this work.

3.6 References

[1] Myerson, A.S. and Ginde, R. *Handbook of Industrial Crystallization,* Edited by Myerson, A. S., Butterworth-Heinemann, Boston, **1993**.

[2] Ingle, J. D.; Crouch, S. R. *Spectrochemical Analysis*, Prentice Hall Inc., **1988**.

[3] Walton, A. G. *Mikrochim. Ichnoanal. Acta,* **1963**, 3, 422-430.

[4] Kerker, M. *Journal of Colloid and Interface Science*, **1987**, 119(2), 602-604.

[5] Watanabe, M.; Nakau, C. *J. Petrol. Mineral and Ore Deposits*, **1929**, 1 61-64.

[6] Chivate, M. R.; Tavare, N. S. *Chemical Engineering Science*, **1975**, 30 (3), 354-355.

[7] Palwe, B. G.; Chivate, M. R.; Tavare, N. S. *Ind. Eng. Chem. Process Dev.*, **1985**, 24 (4), 914-919.

[8] Mullin, A. W. *Crystallization,* 3rd edition, **1993**, Butterworth-Heinemann Ltd., Oxford, London.

[9] Söhnel, O.; Mullin, J. W. *Journal of Crystal Growth*, **1982**, 60 (2), 239-250.

[10] Neilsen, A. E.; Söhnel, O. *Journal of Crystal Growth*, **1971**, 11 (3), 233-242.

Chapter 4

THE EFFECT OF POLYMERIC ADDITIVES ON CALCIUM CARBONATE POLYMORPH FORMATION *

* To be submitted to *Crystal Growth and Design.*

Polycarboxylic acids are well known to affect calcium carbonate crystallization. Agarwal et al.[1] reported previously the synthesis of polymaleimide by a variety of techniques and initiators. In the present work, the effect of these polymers on calcium carbonate crystallization was studied by a variety of techniques. Crystallization experiments were carried out in a one liter LABMAX® automated batch reactor and the concentration of calcium in solution was determined in real time. Raman spectroscopy was used to determine the relative amount of various calcium carbonate polymorphs as the crystallization occurred. However, since Raman spectroscopy is a scattering technique, which may make it surface selective and therefore results from solids may not be representative of bulk of sample. X-ray diffraction (XRD) was used to compare the results obtained by Raman spectroscopy. Peak intensity ratios were used for both Raman spectroscopy and XRD for calibration and measurement purposes. The results obtained by these two techniques for final percent vaterite for calcium carbonate crystallization in presence of polymeric additives were in agreement within two percent. Therefore use of Raman spectroscopy for *in situ* measurement of polymorph composition during calcium carbonate crystallization appears accurate. Scanning electron microscopy (SEM) data was useful in understanding the crystal morphology and to determine crystal size.

4.1 Introduction

Calcium carbonate is used commercially for a variety of applications such as filler for plastic, rubber and paper, glass manufacture and sulfur dioxide scrubbing. [2,3] Fouling of surfaces in industrial equipment is also primarily due to deposition of calcium salts. [4,5,6] Calcium carbonate crystallizes into three different polymorphs: calcite, the rhombohedral polymorph is the thermodynamically most stable form[7] followed by vaterite, which is hexagonal. [7,8,9] and aragonite, the orthorhombic form that is least stable[7,10] and is synthesized by direct precipitation.[11]

The physical properties of the crystallized product depend largely on the percentage of each polymorph present. Furthermore, vaterite and aragonite can also act as precursors to calcite. Therefore, it is necessary to quantify these polymorphs during and after the crystallization process. Numerous techniques have been used for this task, which include infrared spectroscopy (IR), Raman spectroscopy, differential scanning calorimetry (DSC), scanning electron microscopy (SEM) and x-ray diffraction (XRD). [12-15] Among these techniques, IR and Raman are the only suitable ones for *in situ* monitoring. Raman spectroscopy has some advantages over IR, which include minimal sample preparation, ease of remote sensing, and less interference from water.

There have been previous attempts to study the effect of additives on crystallization of calcium carbonate such as in presence of amino acids[16] and surface modifiers,[17] but the focus of these studies was not the effect on polymorph formation. In the present work, Raman spectroscopy was used as a tool for *in situ* monitoring of polymorphs and to monitor the effect of polymaleimide additives[1] on relative percent of these polymorphs.

However, due to Raman being a surface technique; results are typically not representative of bulk of the sample. Therefore there was a need to further compare and confirm the results obtained by Raman technique with other methods. XRD cannot be used for *in situ* measurements but would be an excellent technique to confirm whether the results from Raman spectroscopy are valid for bulk of the crystals formed. Peak intensity ratio would be used to quantify the polymorphs by both Raman spectroscopy and XRD technique.[15] Presence of a small amount of additive greatly influences the crystallization process. Polycarboxylic acids such as polymaleimide greatly affect calcium carbonate crystallization. Authors have previously reported the synthesis and characterization of these maleimide polymers.[1] Various polymeric inhibitors used in the current study are listed in Table 4.1.

4.2 Materials

ACS reagent grade starting materials and solvents were used as received from commercial suppliers without further purification, unless otherwise specified. The calcium selective electrode was purchased from Orion Research, Inc. (model 97-20 ionplus electrode). Maleimide was purchased from TCI America and was recrystallized two times from ethyl acetate before use. Raman spectra were collected with Kaiser Optical Systems, Inc. HoloLab Series 5000 ® instrument equipped with a laser which supplies illumination at 784.8 nm. The crystallization experiments were carried out in a LABMAX ® automated laboratory reactor from ASI-Mettler Toledo. The powder XRD patterns were measured on a Rigaku Rotaflex diffractometer equipped with a rotating anode and a Cu Kα radiation. Photomirographs were recorded with a JEOL JSM-35C scanning electron microscope equipped with a Tracor Northern EDS detector. SEM data were acquired at an accelerating voltage of 20kV.

4.3 Methods

4.3.1 Preparation of pure calcium carbonate polymorphs

Calcite was prepared by dropwise addition of 1 L of 1M ammonium carbonate to 1L of 1M calcium nitrate. The suspension was stirred for fifteen days at room temperature to ensure complete conversion to calcite. Calcite powder was then filtered through 22 μm pore size filter media and washed three times with deionized water at 70°C. The product was dried for 2 days at 110°C.

Vaterite was prepared by adding 500 mL of a 5 mM calcium chloride solution into the same volume of 5 mM sodium carbonate solution. The solutions were adjusted to pH 10

before mixing by a strong acid or base (HCl and NaOH respectively). The mixture was kept well stirred and filtered through 22 μm pore size filter media after 15 minutes of mixing at 25°C. The crystals obtained were washed three times with deionized water and dried for one hour at 110°C.

4.3.2 Polymers used as additives for calcium carbonate crystallization

The polymers used for these crystallization studies have been synthesized by a number of techniques and using a variety of initiator systems. Details for the synthesis of these polymers have been described in chapter 2. Table 4.1 provides a list of polymers used and their properties.

S.No.	Inhibitor	Source	Percent Conversion[1]	C-N Connected Monomer (%)[1]	Molecular Weight[2]
1	PMI_Cu_sys[3]	Synthesized	95.6 ± 0.5	43.2± 0.8	5900± 100
2	PMI_KOH[4]	Synthesized	92.8± 0.3	79.8± 0.9	1100± 180
3	PMI_PbO[5]	Synthesized	99.0± 0.5	38.7± 0.8	11500± 90
4	PAA[6]	Aldrich	-	-	5000
5	PaspAcid[7]	Bayer Corp.	-	-	-
6	Acusol®	Rhom & Haas	-	-	5000

Table 4.1 Properties of the polymers used as additives for crystallization studies.

[1] by ratio of peak integration (mean of three different runs)

[2] M_n by GPC with respect to polyacrylate standards (mean of three different runs)

[3] *PMI_Cu_sys* refers to Polymaleimide synthesized by bis(triphenylphosphine) Cu(I) nitrate and t-butyl benzyl alcohol initiator.

[4] *PMI_KOH* refers to Polymaleimide synthesized by KOH initiator.

[5] *PMI_PbO* refers to Polymaleimide synthesized by PbO and t-butyl benzyl alcohol initiator.

[6] *PAA* refers to Polyacrylic acid.

[7] *PaspAcid* refers to Polyaspartic acid.

4.3.3 *Solution concentration of calcium during batch crystallization*

A series of calcium standards (10-200 ppm as $CaCO_3$) solutions were used to calibrate the calcium selective electrode. A stock solution of 0.01 M $CaCl_2$ (1000 ppm, hardness as $CaCO_3$) was prepared by dissolving 0.1109 g of $CaCl_2$ in 100 mL of milli-Q water and then diluted to give appropriate standard concentrations. The electrode was interfaced to the LABMAX® batch reactor to determine the solution concentration of calcium in real time as the crystallization proceeded, using the calibration curve.

4.3.4 *In situ determination of polymorph concentration by Raman spectroscopy*

The relative amounts of calcite and vaterite were determined in real time as the crystallization proceeded in the LABMAX® automated batch reactor by acquiring a Raman spectrum every ten minutes. The intensity ratio of the vaterite and calcite peaks at 690 and 711 cm^{-1}, respectively, was used to determine the percent of vaterite in the crystals

4.3.5 *Verification of Raman spectroscopy results by XRD*

Samples of calcium carbonate collected after the crystallization were analyzed by XRD to verify the results obtained by Raman spectroscopy. XRD data were collected at rotation speed of 2°/minute. Electron beam was generated at a voltage of 50 kV and 100 mA current. The standards used for calibration were prepared in similar way, as described for Raman experiments. The intensity ratio of vaterite (110 plane) at 24.6° and calcite (104 plane) at 29.1° was used for calibration as well as quantification.

4.4 Results and Discussion

4.4.1 Pure calcium carbonate polymorphs

Synthesis of polymorphs in pure form was one of the critical aspects of the study; therefore, Raman and SEM studies were performed on the pure polymorph samples (calcite and vaterite). These studies confirmed the formation of pure forms of calcite and vaterite as shown in Figure 4.1 and 4.2. Aragonite was also synthesized in pure form, but was not present in any of the crystallization experiments performed at 25°C because aragonite formation has been reported only in crystallizations done at temperatures near 90°C.

4.4.2 Calibration of Raman spectra

A peak intensity ratio was used to calibrate Raman spectra. The intensity ratio of in plane bending modes of carbonate groups in calcite and vaterite, 711 cm^{-1} and 690 cm^{-1}, respectively, was used for the Raman calibration. Figure 4.3 shows the Raman spectra of mixtures obtained by physical mixing of pure calcite and vaterite in different weight ratios. The intensity ratio of peaks at 690 cm^{-1} and 711 cm^{-1} is shown as a function of weight percent vaterite in Figure 4.4. The data were fitted to a second order polynomial to get the calibration equation.[14,15]

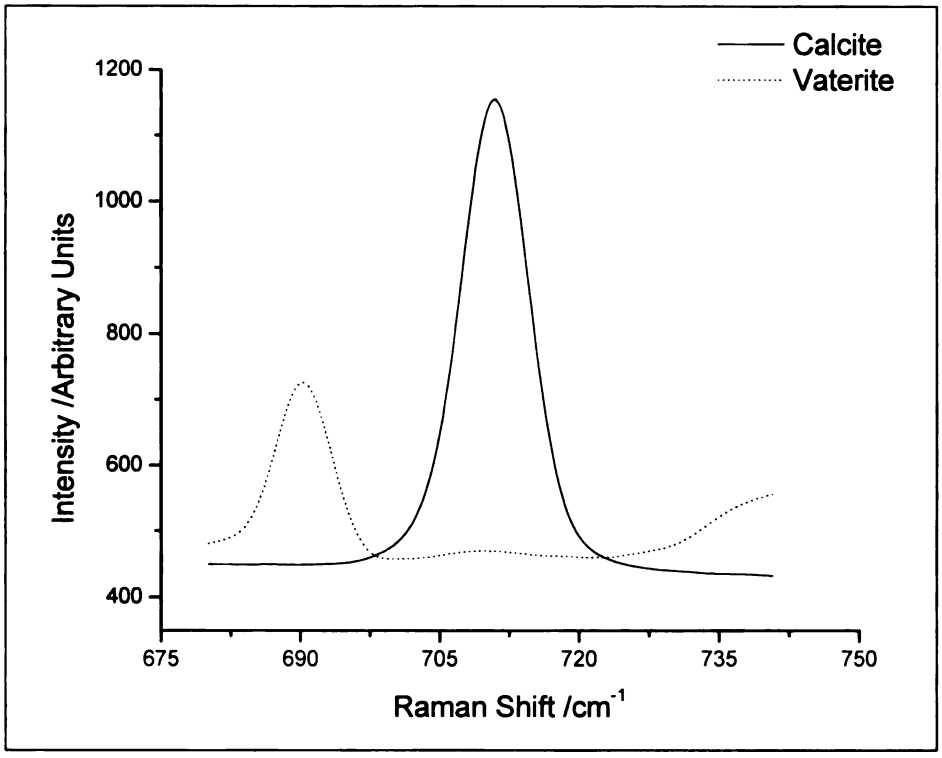

Figure 4.1 Raman spectra of synthesized pure calcite and vaterite.

Experimental conditions : 5 exposures & 5 accumulations

Peak Assignments (Carbonyl in plane bending) : Calcite (711 cm^{-1})

Vaterite (690 cm^{-1})

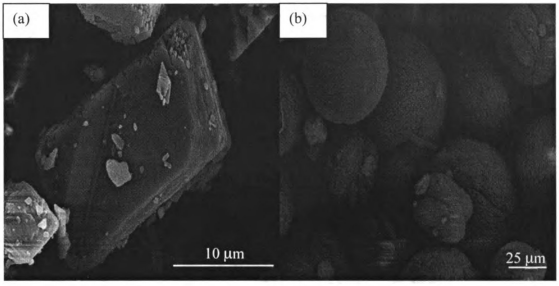

Figure 4.2 SEM images of synthesized pure polymorphs: (a) Calcite (b) Vaterite

Experimental conditions : Gold sputtered samples at accelerating voltage of 20 kV on JEOL JSM-35C scanning electron microscope.

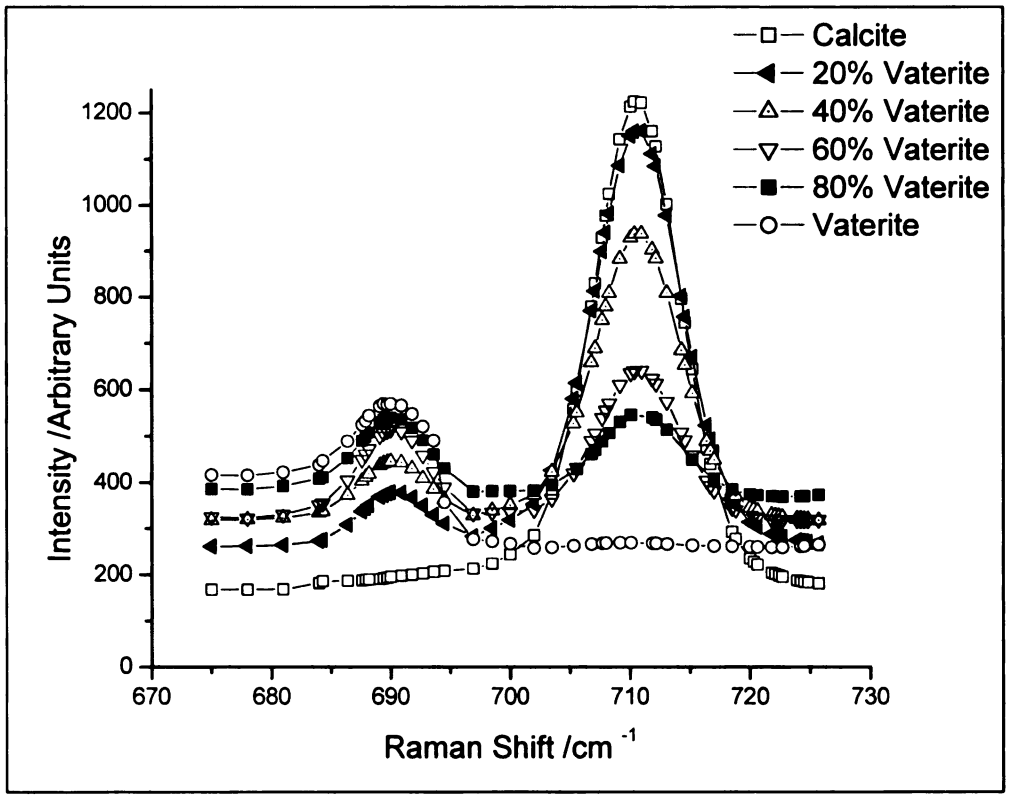

Figure 4.3 Raman spectra of physical mixtures of pure polymorphs showing the variation of intensity of 690 cm^{-1} and 711 cm^{-1} peaks as function of weight percent of vaterite.

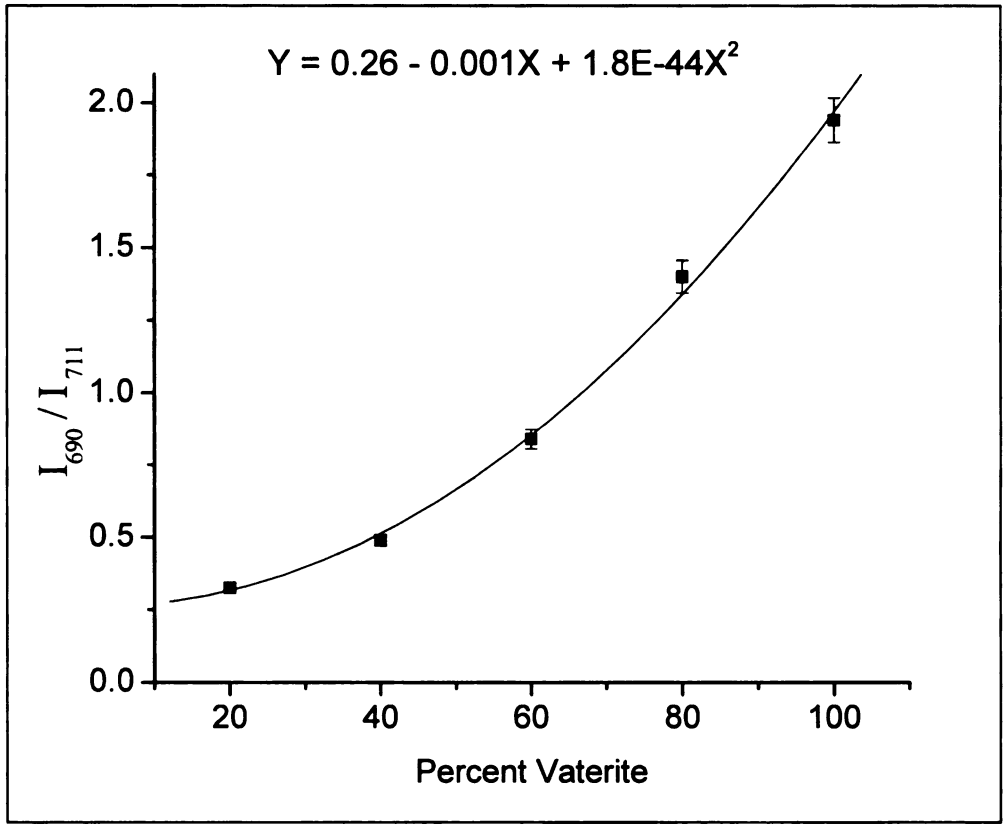

Figure 4.4 Calibration curve obtained by plotting intensity ratio of 690 cm^{-1} and 711 cm^{-1} peaks for Raman spectra of physical mixtures of pure polymorphs.

Error bars represent $\pm\sigma$, N = 4.

4.4.3 Calibration of XRD spectra

Peak intensity ratio was used to calibrate XRD spectra also. Calibration curves similar to that in case of Raman spectroscopy were plotted. The calibration equation obtained was used to convert the final peak intensity ratio to percent vaterite for the calcium carbonate samples obtained after crystallization in presence of various additives. Figure 4.5(a) through 4.5(c) show the XRD curves for the three calcium carbonate polymorphs and their characteristic peaks. Figures 4.6(a) & 4.6(b) shows the variation in intensity of peaks at 24.6° and 29.1° respectively for standard mixtures of calcite and vaterite. The peak at 24.6° was due to the diffraction of x-ray beam by 110-crystal plane of vaterite. Diffraction of x-ray beam by 104-crystal plane of calcite gave the peak at 29.1°. The intensity ratio of these two peaks has been plotted as a function of weight percent vaterite in Figure 4.7. The data was fitted to a first order equation to get the calibration equation for XRD.

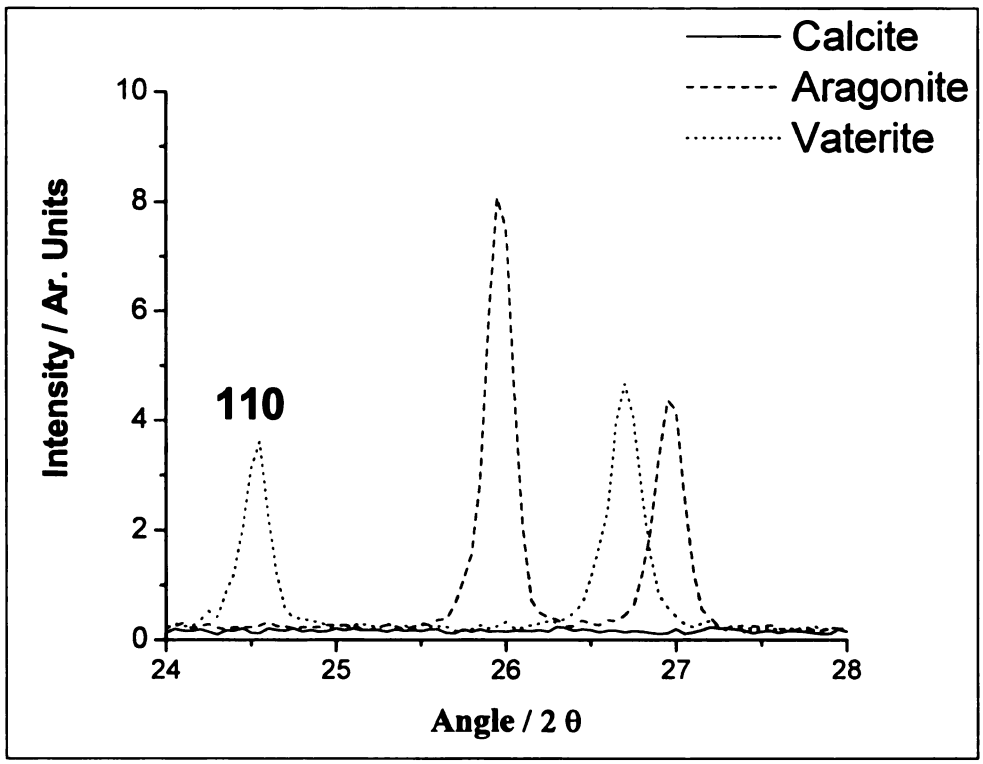

Figure 4.5 (a) XRD of pure calcium carbonate polymorphs showing characteristic peak of vaterite 110 at 24.6°.

Experimental conditions : Scan rate of 2°/min., 2θ/θ-reflectance collection mode.

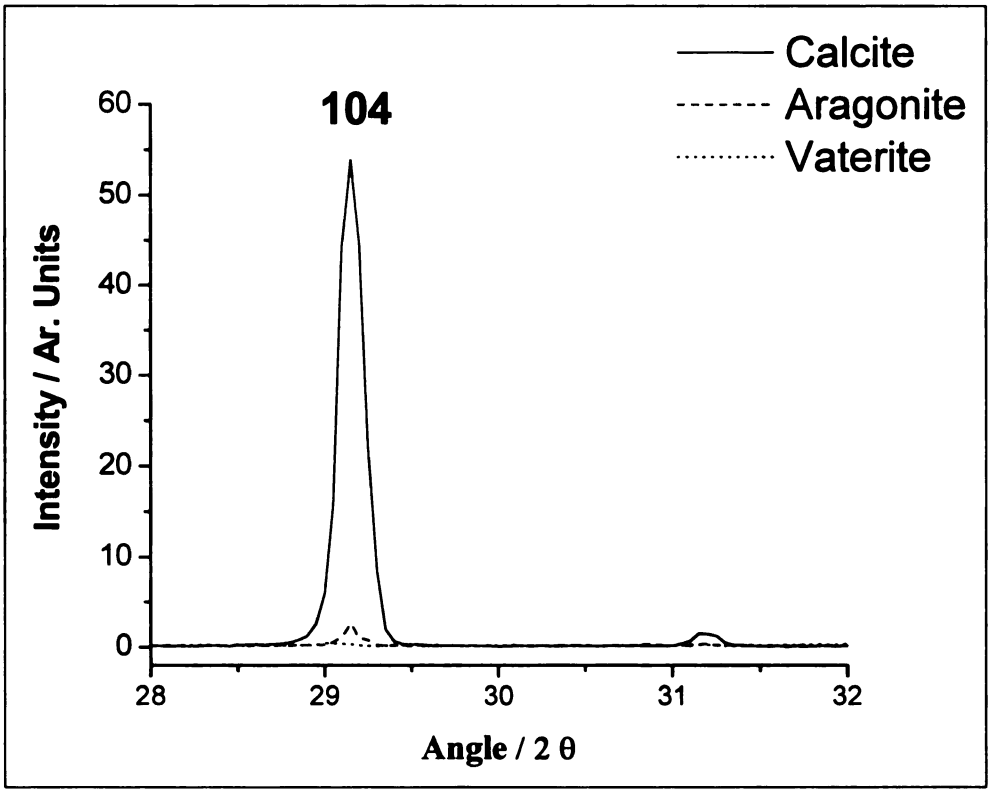

Figure 4.5 (b) XRD of pure calcium carbonate polymorphs showing characteristic peak of Calcite 104 at 24.6°.

Experimental conditions : Scan rate of 2°/min., 2θ/θ-reflectance collection mode.

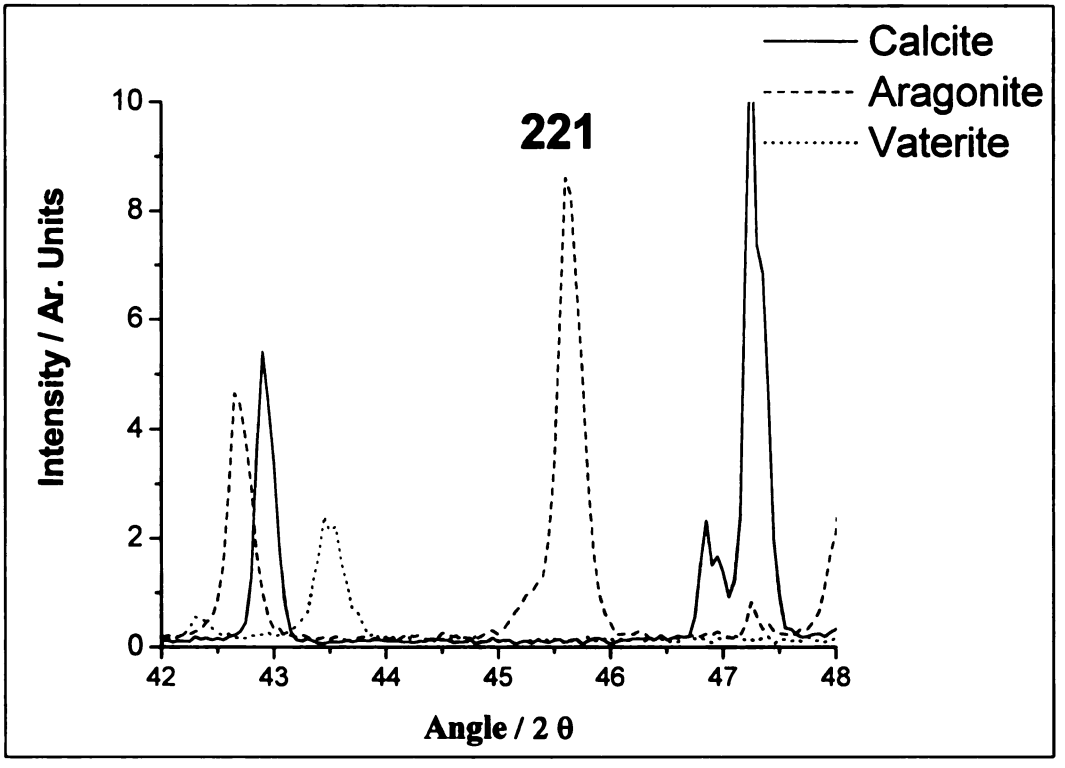

Figure 4.5 (c) XRD of pure calcium carbonate polymorphs showing characteristic peak of Aragonite 221 at 45.7°.

Experimental conditions : Scan rate of 2°/min., 2θ/θ-reflectance collection mode.

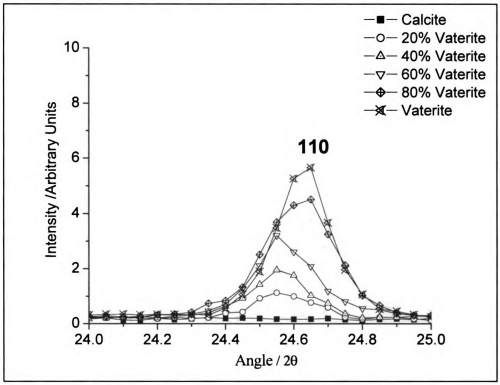

Figure 4.6 (a) XRD pattern of mixtures of pure calcite and vaterite showing the variation in peak intensity due to diffraction by 110 plane at 24.6° as a function of vaterite concentration.

Experimental conditions : Scan rate of 2°/min., 2θ/θ-reflectance collection mode.

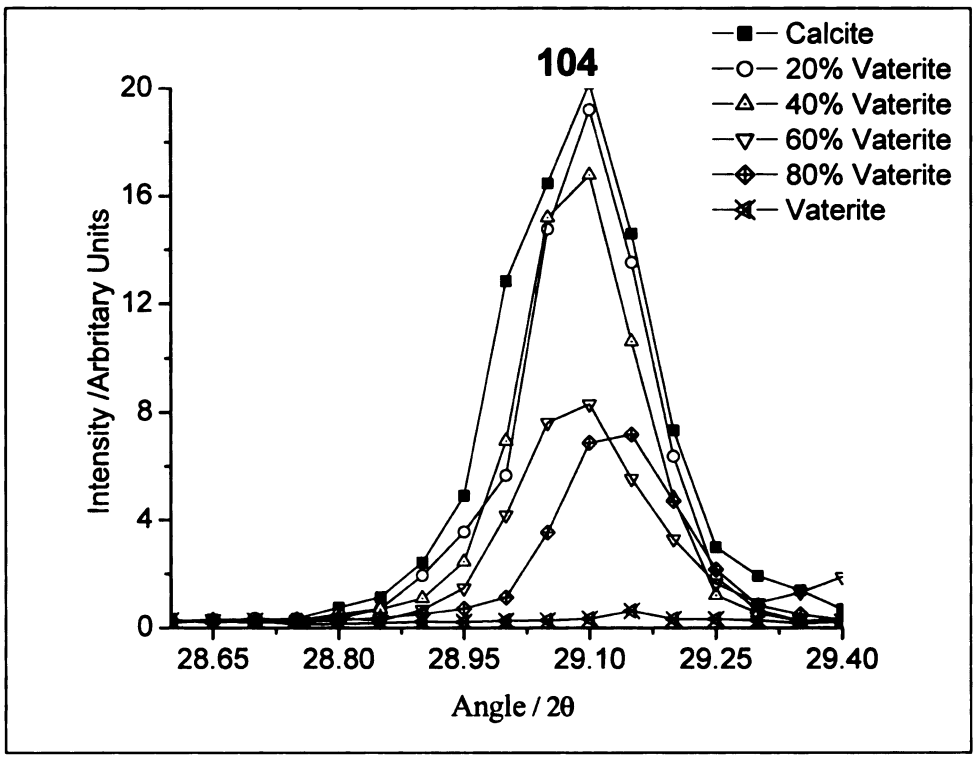

Figure 4.6 (b) XRD pattern of mixtures of pure calcite and vaterite showing the variation in peak intensity due to diffraction by 104 plane at 29.1° as a function of vaterite concentration.

Experimental conditions : Scan rate of 2°/min., 2θ/θ-reflectance collection mode.

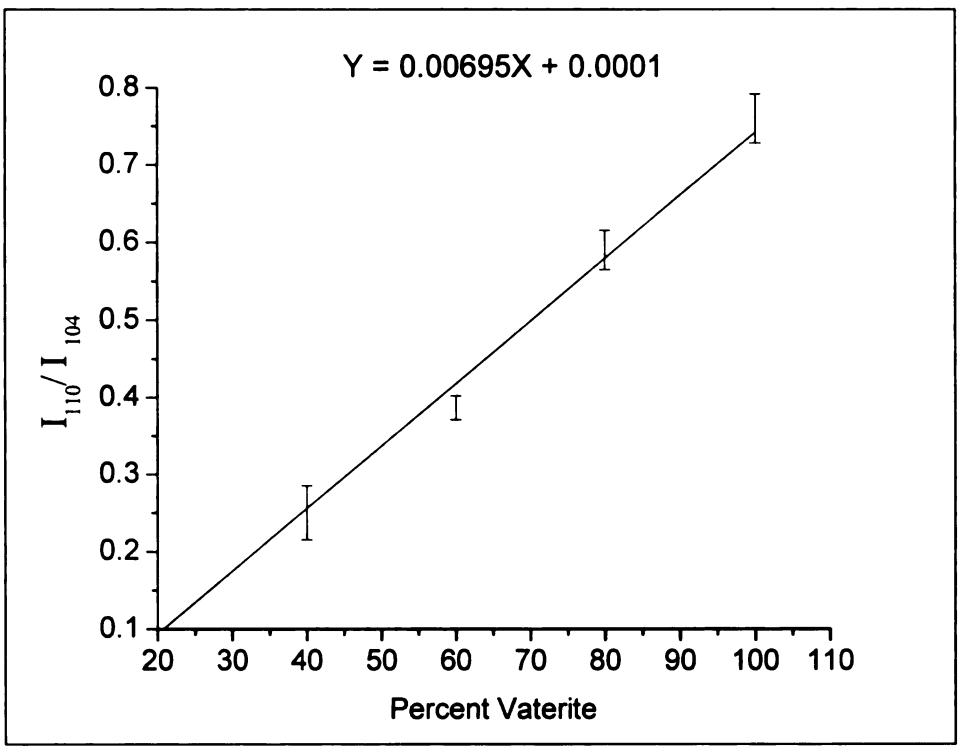

Figure 4.7 Calibration curve obtained by plotting intensity ratio of 110 and 104 diffraction peaks at 24.6° and 29.1° for XRD pattern of mixtures of pure polymorphs (calcite and vaterite).

Error bars represent ±σ, N = 4.

4.4.4 Comparison of Raman and XRD results

Effect of polymeric additives on percent vaterite at the end of crystallization is shown in Table 4.2. Percent vaterite determined by Raman and XRD techniques are in agreement with each other within one to two percent, which justified the use of Raman spectroscopy for *in situ* monitoring of crystallization. This comparison proves that the results obtained by Raman spectroscopy for percent vaterite indeed represent the average percent vaterite for the bulk of the calcium carbonate samples obtained under various experimental conditions.

S.No.	Polymer Added[1]	% Vaterite (by Raman)[2]	% Vaterite (by XRD)[2]	Crystal Size[3] (μm)
1	None	0	0	26.4± 0.3
2	PMI_Cu_sys [4]	45.9± 0.3	44.5± 0.1	29.8± 0.8
3	PMI_KOH initiated	19.3± 0.2	17.7± 0.1	16.5± 0.5
4	PMI_PbO [5]	3.5± 0.2	1.9± 0.1	43.1± 0.3
5	Polyacrylic Acid	98.8± 0.4	99.1± 0.1	5.7± 0.5
6	Polyaspartic Acid	51.5± 0.3	49.6± 0.2	17.3± 0.5
7	Acusol®	99.0± 0.2	98.7± 0.1	14.2± 0.7

Table 4.2 Comparison of ultimate percent vaterite obtained in batch crystallization of calcium carbonate in presence of polymeric additives by Raman and XRD techniques.

[1] Polymer concentration is 1.4 ppm

[2] Mean of three experiments

[3]Determined by SEM, mean of seven measurements

[4] *PMI_Cu_sys* refers to Polymaleimide synthesized by bis(triphenylphosphine) Cu(I) nitrate and t-butyl benzyl alcohol initiator

[5]*PMI_PbO* refers to Polymaleimide synthesized by PbO and t-butyl benzyl alcohol initiator

4.4.5 Calcium concentration profiles from ion selective electrode

The addition of calcium solution was done slowly (54 g of 6250 ppm Ca^{2+} was added at rate of one gram every 5 minutes) to facilitate formation of larger crystals. As shown in Figure 4.8, instantaneous addition of all the calcium required for crystallization lead to very high supersaturation and therefore very small crystal sizes.[18] The effects of polymeric additives were studied under controlled addition of calcium solution. Figure 4.8 shows the calcium concentration profiles during these crystallization experiments. The results indicate there are three different types of effect due to the polymeric additives. Polyacrylic acid and polyaspartic acid do not interfere with the equilibrium solubility of calcium carbonate and the final concentration of calcium in solution is approximately the solubility of calcium carbonate in pure solution. Polymaleimide synthesized using potassium hydroxide or lead oxide with t-butyl benzyl alcohol initiators alters the calcium carbonate solubility. In the presence of either of these two polymers, the normal solubility limit of calcium carbonate is not reached at any point in time, but crystallization proceeded under these conditions, which could only occur if the additives lower the solubility of calcium carbonate. Acusol® and polymaleimide synthesized by bis(triphenylphosphine)-copper(I) nitrate and t-butyl benzyl alcohol initiators represent the third class of polymeric additives studied. In the presence of these polymeric additives, the calcium concentration did not go back to its normal solubility limit at the end of crystallization, which might be due to increased solubility of calcium carbonate.

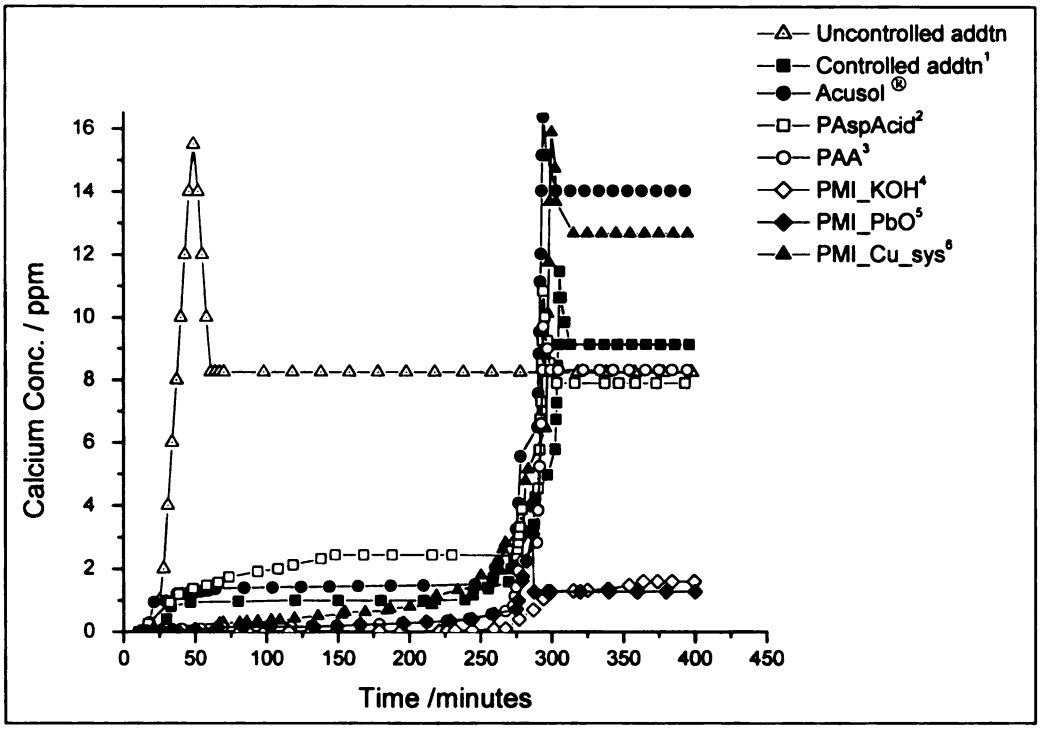

Figure 4.8 Calcium ion concentration during calcium carbonate crystallized in presence of various polymeric additives determined by calcium selective electrode interfaced with LABMAX.®

*Solubility of $CaCO_3$ samples was determined to be 8.2 ppm as Ca^{2+} ions.

[1] 600 ppm Ca^{2+} was added at rate of 0.2mL/minute.

[2] *PaspAcid* refers to Polyaspartic acid

[3] *PAA* refers to Polyacrylic acid

[4] *PMI_KOH* refers to Polymaleimide synthesized by KOH initiator.

[5] *PMI_PbO* refers to Polymaleimide synthesized by PbO and t-butyl benzyl alcohol initiator.

[6] *PMI_Cu_sys* refers to Polymaleimide synthesized by bis(triphenylphosphine) Cu(I) nitrate and t-butyl benzyl alcohol initiator.

4.4.6 Comparison of polymeric additives

As shown in Table 4.2, Acusol® and polyacrylic acid predominantly led to formation of vaterite. Polymaleimide synthesized with the lead oxide/t-butyl benzyl alcohol initiator system did not alter the phase formed and yielded predominantly the calcite form. Polyaspartic acid and the other polymaleimide samples prepared by bis(triphenylphosphine)-copper(I) nitrate/t-butyl benzyl alcohol or potassium hydroxide as initiator affected the phase equilibrium partially. Figure 4.9 shows the variation of the relative amount of vaterite during the crystallization process. Acusol® and polyacrylic acid both form predominantly vaterite form, but in case of Acusol®, calcite was never formed during the course of crystallization. In case of polyacrylic acid, only calcite was formed initially but later vaterite is the predominant form. Crystal sizes determined by SEM are also listed in Table 4.2. Some polymeric additive marginally affected the average crystal size, but polymaleimide prepared by the lead oxide/t-butyl benzyl alcohol initiator system resulted in an increase in crystal size. Polyacrylic acid reduces the crystal size significantly. SEM images of calcium carbonate synthesized in absence and presence of various polymeric additives are shown in Figure 4.10 and 4.11 respectively. Images in Figure 4.11 distinctly show the difference in the relative amount of two polymorphs with change in the kind of polymeric additive.

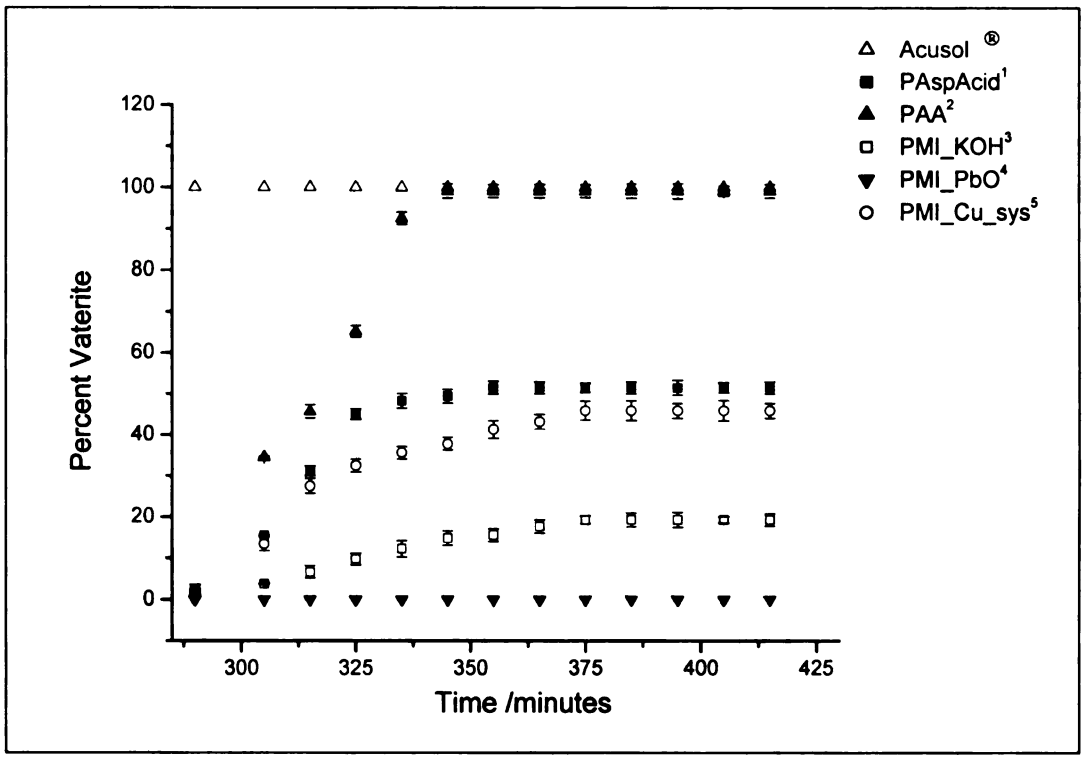

Figure 4.9 Percent vaterite, determined *in situ* during calcium carbonate crystallized in presence of various polymeric additives by Raman spectroscopy.

[1]*PAspAcid*	refers to Polyaspartic acid.
[2]*PAA*	refers to Polyacrylic acid.
[3]*PMI_KOH*	refers to Polymaleimide synthesized by KOH initiator.
[4]*PMI_PbO*	refers to Polymaleimide synthesized by PbO and t-butyl benzyl alcohol initiator.
[5]*PMI_Cu_sys*	refers to Polymaleimide synthesized by bis(triphenylphosphine) Cu(I) nitrate and t-butyl benzyl alcohol initiator.

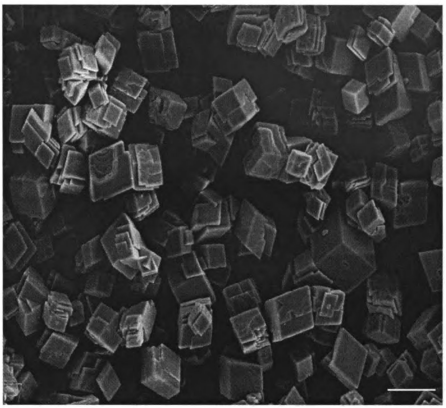

Figure 4.10 SEM image of calcium carbonate crystallized in absence of any polymeric additive.

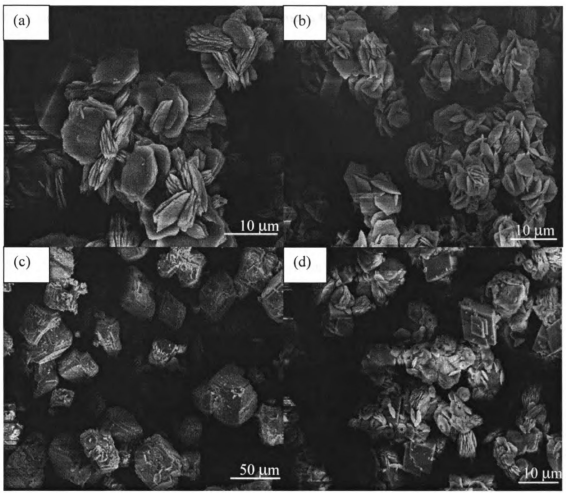

Figure 4.11 SEM images of calcium carbonate crystallized in presence of polymeric additives

(a) Predominantly vaterite formed in presence of Acusol®.

(b) Predominantly vaterite formed in presence of polyacrylic acid.

(c) Predominantly calcite formed in presence of PMI synthesized by PbO-t-butyl benzyl alcohol.

(d) Mixture of vaterite and calcite formed in presence of PMI synthesized using KOH as initiator.

• SEM of remaining two polymeric additives was similar to (d), therefore not shown here.

4.5 Conclusions

The polymeric additives altered the crystallization of calcium carbonate with respect to the kind of polymorph and crystal size. Polymer additives such as Acusol® or polyacrylic acid could be used to form the vaterite phase selectively during synthesis of precipitated calcium carbonate. These additives could also be used to increase the crystal size, which cuts down the cost of downstream processes in an industrial environment. The differences in the properties of PMI synthesized under varying conditions are due to the variations in their molecular weight and the percentage of C-N connected polymers. Polymaleimide synthesized by potassium hydroxide as initiator was not as effective as Acusol® and polyacrylic acid to selectively form vaterite, however it does affect the polymorph equilibrium to certain extent. However, the effect of molecular weight, and importance of percentage of C-N connected monomers present in the polymers require a more thorough study than that reported here. The results obtained by Raman and XRD techniques for final percent vaterite formed in calcium carbonate crystallization in presence of polymeric additives agreed within two percent. Therefore use of Raman spectroscopy for *in situ* measurement of polymorph composition during calcium carbonate crystallization appears accurate. In summary, simple methods for altering the polymorph ratio for calcium carbonate crystallization were reported and the observed effects have important commercial implications.

4.6 Acknowledgements

The author wishes to thank Applied CarboChemicals, Inc. and the Center for New Plant Products and Processes at Michigan State University for financial support of this work. The authors also thank Kaiser Optical Systems Inc. for supplying the Raman Spectrometer used in this study.

4.7 References

[1] Agarwal, P.; Yu, Q.; Harant, A.; Berglund K. A.; *Industrial & Engineering Chemistry Research*, submitted August **2002**.

[2] Rowell, R. M. *Science and Technology of Polymers & Advanced Materials*, Edited by P.N. Prasad *et. al.*, Plenum Press, New York, **1998**, 869-872.

[3] Enomae, T., Proceedings of the *5th Asian Textile Conference*, Kyoto, Japan, **1999,** 1, 464-467.

[4] Walker, C. K.; Frazer, L. C.; Dibrell, B. L., *CORROSION*/94, Houston, **1994,** paper no. 52.

[5] Shaughnessy, C. M., Kline, W. E., *Journal of Petroleum Technology*, **1983**, 35(11), 1783-1791.

[6] Morizot, A., Neville, A., Hodgkiess, T., *Journal of Crystal Growth*, **1999**, 198-199, 738-743.

[7] Leeuw, Nora H. de, Parker Stephen C., *Journal of Physical Chemistry B*, **1998**, 102, 2914-2922.

[8] Litvin, A. L., Samuelson, L. A., Charych, D. H., Spevak, W., Kaplan, D. L., *Journal of Physical Chemistry*, **1995**, 99(32), 12065-1268.

[9] Wong, K. K. W., Brisdon, B. J., Heywood, B. R., Hodson, A. G. W., Mann, S., *Journal of Materials Chemistry*, **1994**, 4(9), 1387-1392.

[10] Archibald, D. D., Qadri, S. B., Gaber, B. P., *Langmuir*, **1996**, 12(2), 538-546.

[11] Davies, P., Dollimore, D., Heal, G. R., *Journal of Thermal Analysis*, **1978**, 13(3), 473-487.

[12] Verges-Belmin, V., *Atmospheric Environment*, **1994**, 28(2), 295-304.

[13] Lal G. K.; Holdren, G. C., *Environmental Science and Technology*, **1981**, 15(4), 386-390.

[14] Kontoyannis, C. G.; Orkoula, M. G.; Koutoukos, P. G., *Analyst*, **1997**, 122, 33-38.

[15] Kontoyannis, C. G.; Vagenas, N. V., *Analyst*, **2000**, 125, 251-255.

[16] Manoli, F.; Kanakis, P.;Malkaj, P.; Dalas, E.; *Journal of Crystal Growth*, **2002**, 1-3, 363-370.

[17] Agnihotri, R.; Mahuli, S. K.; Chauk, S. S.; Fan, L. S., *Industrial Engineering and Chemistry Research*, **1999**, 38, 2283-2291.

[18] Myerson, A.S. and Ginde, R. *Handbook of Industrial Crystallization,* Edited by Myerson, A. S., Butterworth-Heinemann, Boston, **1993**.

Chapter 5

CONCLUSIONS

The research presented in this dissertation focused on two important issues; namely synthesis of polymers by novel methods and evaluation of the effects of these polymeric additives on crystallization of calcium carbonate. Chapter 2 describes synthesis of a variety of polymers by various techniques and their subsequent characterization. The efficiency of these polymers with respect to their use in inhibiting calcium carbonate crystallization was shown in chapter 3. Calcium carbonate crystallization was greatly affected by presence of these polymeric additives. Polymaleimide synthesized by anionic polymerization using potassium hydroxide was the most efficient additive for inhibiting the crystallization of calcium carbonate followed by polyaspartic acid. This inhibition was demonstrated by the longest induction time and highest percent growth inhibition amongst the polymers tested. In general, polymers with nitrogen in the main chain (polymaleimide made by anionic initiation and polyaspartic acid) are more efficient in inhibiting the crystallization of calcium carbonate.

Use of intensity ratio to determine the percent polymorph during calcium carbonate crystallization by Raman spectroscopy has been demonstrated as a very powerful technique for real time measurements and has not been reported for such crystallization system. The polymaleimide polymers reported in chapter 2 of this dissertation were shown to alter the phase of calcium carbonate that formed during the crystallization process. A very small amount (1.4 ppm) of the polyacrylic acid and Acusol® solution caused the calcite-vaterite equilibrium to shift drastically. Polymers with linear C-C main

chain, polyacrylic acid and Acusol®, are more effective in causing habit modification in calcium carbonate. This is due to the fact that linear chains have better adsorption on the growing crystal nuclei and hence changes the equilibrium to a greater extent as shown in chapter 1.

To summarize, a simple method to influence to phase behavior during crystallization has been reported in this study and this effect has great commercial implications in manufacture of precipitated calcium carbonate. Polymaleimide synthesized by anionic polymerization has been demonstrated to perform better than current industrial anti-scaling agents.

Chapter 6

FUTURE WORK

6.1 Introduction

Polymaleimide polymers were shown to have promising properties with respect to their effect on crystallization of calcium carbonate.[1,2] These polymers were also efficient with respect to influencing the phase equilibrium of polymorphs in the crystallization process. Future research on the synthesis of these polymers should involve finding better initiator systems that are industrially viable and are environmentally benign. Raman spectroscopy was used as a tool for *in situ* monitoring of the crystallization process. However the '*modus operandi*' of these additives for influencing the phase behavior is yet not known, although data indicates that they do modify the habit of crystals by adsorption to specific crystal faces. Further studies should investigate this mode of action in greater detail.

6.2 Proposed Studies

6.2.1 Synthesis of maleimide polymers

Some of the polymer syntheses reported in chapter 2 were very useful to study the structure property relationship for these maleimide polymers and demonstrate their efficiency for use as anti-redeposition and anti-scaling agents[3] and to influence the phase behavior during the crystallization process. However, some of these initiators such as the lead oxide-alcohol system are not suitable for commercial application. Therefore additional metal compounds should be screened for their efficiency in polymerization of

maleimide. Scale up of such polymerization reactions needs to be undertaken in the future for this technology to have useful implications.

6.2.2 Production of precipitated calcium carbonate (PCC) in the presence of polymeric additives

The polymaleimide polymers have been shown to be very efficient in influencing the phase equilibrium for calcium carbonate crystallization in batch crystallization.[2] The importance of PCC in the polymer and paper industries[4] was emphasized in chapter 1. It is proposed to study the efficacy of using these additives in real industrial environment to influence the phase formed during the production of PCC.

6.2.3 Insight into habit modification of calcium carbonate crystallization

There are indications that the influence of the polymeric additives on habit modification is by adsorption onto crystal faces during the crystallization process but the details are not very clear. The effect of additives needs to be further explored by various studies. One such study could involve variation in the moment these additives are added to the reaction mixture. Another study could focus on use of other kinds of additives such as epoxysuccinic acid derivatives of amino acid on calcium carbonate crystallization.[5]

6.3 References

[1] Agarwal, P.; Yu, Q.; Harant, A.; Berglund K. A.; *Industrial & Engineering Chemistry Research*, submitted August **2002**.

[2] Agarwal, P.; Berglund, K. A. to be submitted to *Crystal Growth and Design.*

[3] Freeman, M. B.; Paik, Y. H.; Swift, G.; Wilczynski, R.; Wolk, S. K.; Yocum, K. M. *ACS Symp. Series 626, American Chemical Society: Washington, DC*, **1996**, 118-136

[4] http://www.ibase093.eunet.be/en/ccawhat.html

[5] Ngowe, C. O. *Synthesis and Characterization of Tailor-made Additives for Inhibition of Sparingly Soluble Calcium Salt Crystallization*, Ph. D. dissertation, **2002,** Department of Chemistry, Michigan State University

APPENDIX

Volume of inhibitor (mL)	PMI_KOH-initiated	PMI_CuTPP-ROH	PAA (M. W. 1200)	Acusol®	PMI_PbO-ROH
0.00	126.88	130.43	123.33	123.33	123.23
0.50	116.22	123.33	112.67	116.22	108.58
1.00	109.11	112.67	102.00	105.56	92.45
1.50	98.45	105.56	91.34	94.90	78.96
2.00	84.24	98.45	80.68	84.24	66.70
2.50	73.57	87.79	66.47	73.57	47.80
3.00	62.91	80.68	52.25	59.36	33.23
3.50	52.25	70.02	34.48	45.15	20.45
4.00	41.59	62.91	16.72	30.93	7.68
4.50	30.93	52.25		16.72	
5.00	16.72	41.59		2.50	
5.50	6.06				
6.00					
6.50					

Table A.1 Data for Figure 2.5 Chelation studies of polymers to determine their effectiveness as anti-scaling agent using calcium selective electrode.

Raman shift (cm^{-1})	Calcite	Vaterite	Raman shift (cm^{-1})	Calcite	Vaterite
680.1	4495.8	4806.6	690.3	4490.5	7258.7
680.4	4496.1	4817.1	690.6	4491.4	7232.1
680.7	4496.4	4827.8	690.9	4492.4	7195.2
681	4496.6	4838.9	691.2	4493.8	7121
681.3	4496.8	4850.2	691.5	4495.2	7033.4
681.6	4496.8	4862.6	691.8	4496.8	6922.5
681.9	4496.6	4875.7	692.1	4498.4	6795.5
682.2	4496.2	4890.7	692.4	4499.9	6657.3
682.5	4495.7	4908	692.7	4501.5	6505.2
682.8	4495.1	4927.8	693	4503.1	6349.7
683.1	4494.6	4953.2	693.3	4504.7	6188.2
683.4	4494	4980.8	693.6	4506.5	6027.5
683.7	4493.7	5019.4	693.9	4508.6	5868.8
684	4493.5	5061.3	694.2	4511.1	5715.5
684.3	4493.6	5116.3	694.5	4513.9	5567.3
684.6	4493.8	5179	694.8	4517.8	5431.1
684.9	4494.2	5253.3	695.1	4521.9	5298.9
685.2	4494.7	5341.5	695.4	4527.8	5185.6
685.5	4495.2	5437.8	695.7	4534.1	5077.1
685.8	4495.7	5553	696	4542	4985.1
686.1	4496.2	5673.1	696.3	4551	4902.2
686.4	4496.4	5811.2	696.6	4561.1	4830.9
686.7	4496.4	5953.5	696.9	4572.9	4772.4
687	4496.2	6105.2	697.2	4585.3	4720.1
687.3	4495.7	6259.3	697.5	4599.9	4682.8
687.6	4495	6415.6	697.8	4615	4648.9
687.9	4494.1	6566.6	698.1	4632.2	4626.5
688.2	4493.1	6716.1	698.4	4650.4	4607.8
688.5	4492.2	6846.8	698.7	4670.4	4595.5
688.8	4491.2	6970.6	699	4692.4	4587.2
689.1	4490.6	7070.6	699.3	4715.7	4581.5
689.4	4490.1	7152.9	699.6	4742.7	4579.3
689.7	4489.9	7213.4	699.9	4770.8	4577.8
690	4490.1	7243.3	700.2	4804.4	4578.1

Table A.2 Data for Figure 4.1 Raman spectra of mixtures of pure polymorphs showing the variation of intensity of 690 cm^{-1} and 711 cm^{-1} peaks as function of weight percent of vaterite.

Raman shift (cm^{-1})	Calcite	Vaterite	Raman shift (cm^{-1})	Calcite	Vaterite
700.5	4840.3	4578.6	710.7	11529.0	4696.9
700.8	4881.5	4579.6	711.0	11559.0	4695.2
701.1	4928.1	4580.7	711.3	11504.0	4692.5
701.4	4979.2	4581.8	711.6	11427.0	4689.7
701.7	5040.0	4583.1	711.9	11289.0	4686.2
702.0	5103.8	4584.5	712.2	11114.0	4682.4
702.3	5183.2	4586.5	712.5	10902.0	4678.3
702.6	5267.1	4588.6	712.8	10647.0	4673.9
702.9	5365.8	4591.6	713.1	10376.0	4669.4
703.2	5475.5	4595.1	713.4	10062.0	4664.7
703.5	5597.6	4599.3	713.7	9742.7	4660.1
703.8	5739.4	4604.3	714.0	9402.2	4655.5
704.1	5889.3	4609.8	714.3	9057.4	4651.1
704.4	6069.4	4616.1	714.6	8707.5	4646.8
704.7	6257.7	4622.7	714.9	8361.6	4642.9
705.0	6475.2	4629.7	715.2	8017.5	4639.1
705.3	6707.9	4636.8	715.5	7690.4	4635.9
705.6	6962.4	4643.9	715.8	7369.3	4632.9
705.9	7239.9	4650.8	716.1	7071.3	4630.4
706.2	7530.0	4657.6	716.4	6787.4	4628.2
706.5	7846.9	4663.8	716.7	6523.4	4626.3
706.8	8169.9	4669.8	717.0	6283.9	4624.8
707.1	8511.3	4675.1	717.3	6057.2	4623.4
707.4	8855.2	4680.0	717.6	5864.3	4622.2
707.7	9203.8	4684.3	717.9	5680.1	4621.0
708.0	9546.5	4688.1	718.2	5526.6	4619.7
708.3	9885.2	4691.5	718.5	5385.2	4618.4
708.6	10199.0	4694.1	718.8	5263.4	4616.9
708.9	10506.0	4696.4	719.1	5158.5	4615.1
709.2	10767.0	4697.8	719.4	5063.9	4613.2
709.5	11009.0	4698.9	719.7	4988.2	4611.0
709.8	11205.0	4699.3	720.0	4917.3	4608.7
710.1	11359.0	4699.1	720.3	4861.6	4606.3
710.4	11478.0	4698.4	720.6	4810.5	4604.0

Table A.2 (contd.) Data for Figure 4.1 Raman spectra of mixtures of pure polymorphs showing the variation of intensity of 690 cm^{-1} and 711 cm^{-1} peaks as function of weight percent of vaterite.

Raman shift (cm^{-1})	Calcite	Vaterite	Raman shift (cm^{-1})	Calcite	Vaterite
720.9	4767.6	4601.8	730.5	4397.8	4813.5
721.2	4730.4	4600.0	730.8	4394.9	4833.0
721.5	4696.9	4598.5	731.1	4392.0	4853.1
721.8	4669.2	4597.9	731.4	4388.9	4875.5
722.1	4643.0	4597.5	731.7	4385.8	4899.2
722.4	4621.3	4598.5	732.0	4382.5	4924.2
722.7	4600.9	4600.0	732.3	4379.3	4950.9
723.0	4582.9	4602.6	732.6	4376.0	4978.3
723.3	4566.6	4605.9	732.9	4372.8	5007.3
723.6	4551.5	4609.9	733.2	4369.7	5036.6
723.9	4538.3	4614.9	733.5	4366.9	5066.5
724.2	4525.5	4620.2	733.8	4364.3	5096.6
724.5	4514.3	4626.4	734.1	4362.0	5126.7
724.8	4503.6	4632.7	734.4	4360.1	5156.4
725.1	4493.8	4639.4	734.7	4358.4	5185.9
725.4	4484.6	4646.2	735.0	4357.3	5214.3
725.7	4475.9	4653.1	735.3	4356.4	5242.3
726.0	4467.9	4660.1	735.6	4355.7	5269.1
726.3	4460.1	4667.1	735.9	4355.2	5294.9
726.6	4453.2	4674.2	736.2	4354.8	5319.8
726.9	4446.4	4681.3	736.5	4354.3	5343.3
727.2	4440.3	4688.7	736.8	4353.9	5366.2
727.5	4434.6	4696.3	737.1	4353.0	5387.0
727.8	4429.3	4704.1	737.4	4352.1	5407.4
728.1	4424.6	4712.6	737.7	4350.7	5426.2
728.4	4420.1	4721.4	738.0	4349.1	5444.0
728.7	4416.3	4731.4	738.3	4347.1	5460.7
729.0	4412.7	4742.0	738.6	4344.8	5475.9
729.3	4409.4	4753.8	738.9	4342.3	5490.6
729.6	4406.4	4766.8	739.2	4339.6	5503.5
729.9	4403.4	4780.9	739.5	4336.9	5515.9
730.2	4400.6	4796.9	739.8	4334.3	5527.1

Table A.2 (contd.) Data for Figure 4.1 Raman spectra of mixtures of pure polymorphs showing the variation of intensity of 690 cm^{-1} and 711 cm^{-1} peaks as function of weight percent of vaterite.

Raman shift (cm^{-1})	Calcite	20 % Vaterite	40 % Vaterite	60 % Vaterite	80 % Vaterite	Vaterite
675.0	1684.4	2618.9	3186.8	3254.0	3861.3	4161.3
678.0	1679.5	2625.3	3200.4	3225.8	3853.7	4153.7
681.0	1693.3	2645.4	3236.3	3308.9	3924.7	4224.7
684.0	1823.7	2733.0	3352.2	3510.4	4084.8	4384.8
684.3	1861.9	2758.7	3380.4	3549.7	4116.5	4466.5
686.4	2361.5	3085.4	3732.3	4046.0	4526.3	4886.3
687.6	2800.4	3370.6	4036.4	4494.3	4894.8	5244.8
687.9	2910.5	3442.8	4112.6	4608.8	4987.6	5327.6
688.2	3019.4	3514.4	4187.9	4722.4	5079.6	5439.6
689.1	3281.1	3689.5	4367.4	4996.6	5296.5	5646.5
689.4	3343.7	3732.3	4409.4	5061.3	5346.1	5696.1
689.7	3391.5	3765.6	4440.5	5109.5	5381.8	5681.8
690.0	3418.7	3785.2	4456.3	5134.4	5398.1	5698.1
690.9	3408.3	3782.2	4435.0	5103.6	5359.9	5659.9
691.8	3250.6	3676.7	4300.9	4900.7	5180.7	5480.7
692.7	3000.5	3504.1	4094.1	4588.4	4912.0	5212.0
693.6	2713.9	3303.4	3857.6	4232.9	4606.6	4906.6
694.5	2442.1	3112.6	3632.3	3894.6	4312.5	3567.3
696.9	2030.5	2835.8	3285.0	3332.5	3802.2	2772.4
698.5	2238.2	3010.2	3398.4	3350.9	3807.4	2725.4
700.0	2446.0	3184.6	3511.8	3369.3	3812.5	2678.5
702.0	2861.4	3533.3	3738.5	3406.0	3822.8	2584.5
703.5	3755.0	4265.0	4229.2	3647.9	3947.5	2599.3
705.3	5581.9	5802.7	5272.8	4193.8	4296.5	2636.8
705.6	5979.0	6141.2	5505.4	4317.6	4612.2	2669.8
706.8	7798.5	7702.6	6590.3	4898.2	4702.3	2684.3
707.1	8296.3	8132.0	6892.2	5060.2	4885.6	2688.1
707.7	9291.8	8993.4	7500.5	5386.9	5066.7	2697.8
708.0	9774.6	9412.7	7798.4	5546.9	5300.5	2699.1
708.3	10247.0	9824.0	8091.2	5704.3	5453.1	2686.2
709.2	11426.0	10860.0	8834.6	6104.8	5405.6	2682.4
710.1	12128.0	11496.0	9295.3	6355.3	5352.6	2669.4
710.4	12237.0	11602.0	9373.1	6398.7	5137.0	2639.1
711.0	12216.0	11609.0	9382.5	6408.0	4493.5	2624.8

Table A.3 Data for Figure 4.3 Raman spectra of mixtures of pure polymorphs showing the variation of intensity of 690 cm^{-1} and 711 cm^{-1} peaks as function of weight percent of vaterite.

Raman shift (cm^{-1})	Calcite	20 % Vaterite	40 % Vaterite	60 % Vaterite	80 % Vaterite	Vaterite
711.9	11601.0	11115.0	9034.5	6229.9	4056.1	2618.4
712.2	11276.0	10845.0	8843.3	6130.3	3845.2	2608.7
713.1	10016.0	9780.9	8089.1	5735.0	3744.7	2604.0
714.3	7964.3	8020.4	6845.9	5077.8	3723.7	2597.9
714.6	7444.3	7571.3	6529.9	4910.1	3698.6	2600.0
715.2	6445.0	6706.0	5922.6	4587.1	3690.5	2620.2
716.4	4748.4	5231.4	4892.9	4038.5	3698.1	2626.4
716.7	4397.1	4925.5	4680.0	3925.1	3703.3	2653.1
717.0	4082.5	4651.3	4489.6	3823.7	3731.5	
718.5	2933.4	3648.2	3796.7	3455.7		
718.8	2781.7	3515.7	3706.1	3407.8		
720.0	2354.3	3143.6	3455.8	3276.8		
720.3	2285.9	3085.0	3417.6	3257.4		
720.6	2222.9	3031.3	3382.8	3240.0		
721.8	2047.0	2886.0	3292.0	3199.7		
722.1	2013.8	2859.5	3275.9	3194.0		
722.4	1986.1	2837.5	3262.7	3190.6		
722.7	1959.8	2816.7	3250.2	3187.8		
723.9	1880.4	2751.1	3211.3	3185.4		
724.2	1864.9	2737.3	3203.4	3185.9		
724.5	1852.4	2725.1	3196.7	3186.7		
724.8	1840.6	2713.4	3190.4	3187.4		
725.7	1813.9	2684.5	3176.9	3189.7		

Table A.3 (Contd.) Data for Figure 4.3 Raman spectra of mixtures of pure polymorphs showing the variation of intensity of 690 cm^{-1} and 711 cm^{-1} peaks as function of weight percent of vaterite.

Percent vaterite	I_{690} / I_{711}	Standard deviation
20	0.32	0.01
40	0.49	0.02
60	0.84	0.03
80	1.40	0.06
100	1.94	0.08

Table A.4 Data for Figure 4.4 Calibration curve obtained by plotting intensity ratio of 690 cm^{-1} and 711 cm^{-1} peaks for Raman spectra of mixtures of pure polymorphs.

Angle (degree)	Calcite	Aragonite	Vaterite	Angle (degree)	Calcite	Aragonite	Vaterite
20.0	18.0	25.0	35.0	21.75	17.0	27.0	33.0
20.1	17.0	21.0	35.0	21.8	19.0	24.0	29.0
20.15	25.0	34.0	31.0	21.85	24.0	27.0	30.0
20.2	27.0	22.0	33.0	21.9	25.0	34.0	34.0
20.25	17.0	31.0	34.0	21.95	18.0	29.0	30.0
20.3	25.0	35.0	28.0	22.0	24.0	43.0	27.0
20.35	21.0	40.0	31.0	22.05	25.0	38.0	28.0
20.4	30.0	28.0	30.0	22.1	25.0	38.0	31.0
20.45	25.0	25.0	35.0	22.15	24.0	35.0	29.0
20.5	29.0	24.0	57.0	22.2	15.0	36.0	24.0
20.55	19.0	31.0	54.0	22.25	16.0	30.0	25.0
20.6	23.0	28.0	86.0	22.3	19.0	25.0	25.0
20.65	33.0	27.0	126.0	22.35	28.0	21.0	29.0
20.7	27.0	33.0	99.0	22.4	25.0	30.0	34.0
20.75	20.0	38.0	57.0	22.45	19.0	30.0	26.0
20.8	18.0	55.0	42.0	22.5	28.0	22.0	20.0
20.85	27.0	75.0	42.0	22.55	27.0	30.0	20.0
20.9	22.0	73.0	28.0	22.6	35.0	23.0	30.0
20.95	21.0	61.0	35.0	22.65	51.0	29.0	34.0
21.0	24.0	39.0	27.0	22.7	86.0	33.0	29.0
21.05	23.0	30.0	36.0	22.75	126.0	28.0	60.0
21.1	27.0	27.0	27.0	22.8	353.0	28.0	46.0
21.15	30.0	32.0	30.0	22.85	427.0	34.0	35.0
21.2	17.0	27.0	31.0	22.9	318.0	19.0	29.0
21.25	23.0	31.0	25.0	22.95	149.0	30.0	30.0
21.3	19.0	25.0	37.0	23.0	47.0	33.0	28.0
21.35	20.0	35.0	31.0	23.05	21.0	17.0	28.0
21.4	27.0	33.0	31.0	23.1	22.0	31.0	28.0
21.45	29.0	22.0	24.0	23.15	21.0	31.0	23.0
21.5	15.0	25.0	26.0	23.2	20.0	29.0	26.0
21.55	22.0	25.0	28.0	23.25	15.0	25.0	32.0
21.6	17.0	22.0	29.0	23.3	21.0	23.0	18.0
21.65	22.0	27.0	33.0	23.35	19.0	32.0	27.0
21.7	19.0	24.0	22.0	23.4	21.0	24.0	28.0

Table A.5 Data for Figure 4.5 (a) XRD of pure calcium carbonate polymorphs showing characteristic peak of vaterite 110 at 24.6°.

Angle (degree)	Calcite	Aragonite	Vaterite	Angle (degree)	Calcite	Aragonite	Vaterite
23.45	19	30	32	25.15	18	19	29
23.5	20	27	19	25.20	18	18	27
23.55	17	26	23	25.25	18	23	21
23.6	25	25	19	25.30	15	27	32
23.65	23	28	29	25.35	19	25	20
23.70	25	17	23	25.40	17	20	28
23.75	17	18	17	25.45	18	23	18
23.8	19	34	24	25.50	16	31	28
23.85	22	23	22	25.55	19	27	25
23.9	20	27	27	25.60	19	37	25
23.95	18	28	27	25.65	13	38	24
24.00	13	22	20	25.70	12	65	17
24.05	20	25	31	25.75	19	109	17
24.10	17	31	25	25.80	15	158	19
24.15	16	21	25	25.85	19	291	27
24.20	19	25	36	25.90	15	581	21
24.25	15	29	53	25.95	16	808	25
24.30	10	22	41	26.00	15	752	33
24.35	17	19	86	26.05	17	452	21
24.40	17	23	121	26.10	17	205	22
24.45	21	23	203	26.15	16	71	27
24.50	13	23	313	26.20	18	49	30
24.55	12	26	361	26.25	15	41	34
24.60	21	33	227	26.30	24	37	32
24.65	18	25	120	26.35	22	25	39
24.70	17	25	55	26.40	17	25	49
24.75	21	21	40	26.45	19	36	67
24.80	15	23	39	26.50	18	29	114
24.85	18	23	35	26.55	14	27	171
24.90	15	23	32	26.60	17	36	237
24.95	16	27	27	26.65	17	35	397
25.00	21	27	17	26.70	14	45	467
25.05	18	27	23	26.75	16	61	407
25.10	21	27	28	26.80	15	121	265

Table A.5 (Contd.) Data for Figure 4.5 (a) XRD of pure calcium carbonate polymorphs showing characteristic peak of vaterite 110 at 24.6°.

Angle (degree)	Calcite	Aragonite	Vaterite	Angle (degree)	Calcite	Aragonite	Vaterite
26.95	12	437	59	27.5	15	24	22
27	20	419	43	27.55	17	27	21
27.05	11	258	29	27.6	13	21	19
27.1	14	125	23	27.65	16	15	21
27.15	18	55	31	27.7	16	18	20
27.2	23	41	35	27.75	15	25	15
27.25	21	23	23	27.8	13	18	27
27.3	21	21	17	27.85	11	17	18
27.35	19	30	21	27.9	11	21	22
27.4	17	14	28	27.95	19	21	21
27.45	12	26	16	28	15	15	20

Table A.5 (Contd.) Data for Figure 4.5 (a) XRD of pure calcium carbonate polymorphs showing characteristic peak of vaterite 110 at 24.6°.

Angle (degree)	Calcite	Aragonite	Vaterite	Angle (degree)	Calcite	Aragonite	Vaterite
28	15	15	20	29.8	16	16	21
28.05	16	20	21	29.85	19	17	21
28.1	13	22	13	29.9	17	15	17
28.15	14	18	15	29.95	17	17	23
28.2	13	18	25	30	10	14	18
28.25	14	13	19	30.05	13	16	21
28.3	17	19	24	30.1	15	19	26
28.35	19	19	25	30.15	17	16	13
28.4	20	16	21	30.2	14	15	24
28.45	12	22	23	30.25	19	15	17
28.5	22	26	19	30.3	13	13	23
28.55	31	17	15	30.35	13	23	17
28.6	29	18	21	30.4	17	17	23
28.65	27	21	27	30.45	15	19	18
28.7	35	23	17	30.5	12	22	18
28.75	39	23	19	30.55	13	16	14
28.8	53	16	19	30.6	13	16	21
28.85	80	25	23	30.65	21	15	18
28.9	125	22	23	30.7	21	15	19
28.95	256	30	23	30.75	15	21	23
29	595	27	45	30.8	19	28	16
29.05	1574	55	41	30.85	15	30	17
29.1	4430	117	38	30.9	15	29	21
29.15	5383	263	34	30.95	15	20	12
29.2	4463	101	23	31	15	19	17
29.25	2219	81	15	31.05	37	27	19
29.3	859	23	12	31.1	69	17	26
29.35	195	19	21	31.15	151	29	27
29.4	68	19	27	31.2	145	37	27
29.45	35	21	23	31.25	125	21	22
29.5	29	11	25	31.3	47	25	17
29.55	32	20	22	31.35	23	19	15
29.6	24	15	16	31.4	23	15	19
29.65	17	17	25	31.45	11	15	28
29.7	18	21	15	31.5	16	13	18
29.75	19	16	18	31.55	9	21	21

Table A.6 Data for Figure 4.5 (b) XRD of pure calcium carbonate polymorphs showing characteristic peak of Calcite 104 at 24.6°.

Angle (degree)	Calcite	Aragonite	Vaterite	Angle (degree)	Calcite	Aragonite	Vaterite
42	13	17	15	43.8	12	19	39
42.05	12	21	16	43.85	11	12	20
42.1	9	22	16	43.9	14	16	27
42.15	11	19	19	43.95	13	15	13
42.2	11	23	24	44	11	15	19
42.25	10	24	34	44.05	11	16	21
42.3	19	29	55	44.1	11	13	10
42.35	14	32	53	44.15	9	19	19
42.4	17	45	46	44.2	9	23	18
42.45	13	54	35	44.25	8	19	10
42.5	16	87	26	44.3	11	22	9
42.55	13	151	21	44.35	10	15	13
42.6	19	288	25	44.4	15	13	11
42.65	22	466	17	44.45	14	13	11
42.7	28	445	17	44.5	13	26	14
42.75	45	383	16	44.55	13	23	17
42.8	128	295	21	44.6	8	19	13
42.85	358	171	21	44.65	9	22	18
42.9	541	101	23	44.7	9	17	11
42.95	450	57	27	44.75	14	17	9
43	340	33	18	44.8	6	15	21
43.05	184	34	23	44.85	10	20	8
43.1	79	18	25	44.9	10	27	11
43.15	29	22	31	44.95	17	31	12
43.2	13	18	39	45	9	23	12
43.25	11	23	51	45.05	13	33	10
43.3	15	18	63	45.1	13	48	14
43.35	11	15	121	45.15	5	63	6
43.4	7	15	169	45.2	9	76	9
43.45	7	18	241	45.25	11	95	14
43.5	9	15	213	45.3	7	101	11
43.55	9	19	222	45.35	13	117	14
43.6	9	17	159	45.4	10	129	15
43.65	12	11	117	45.45	8	198	12
43.7	9	14	70	45.5	12	330	15

Table A.7 Data for Figure 4.5 (c) XRD of pure calcium carbonate polymorphs showing characteristic peak of Aragonite 221 at 45.7°.

Angle (degree)	Calcite	Aragonite	Vaterite	Angle (degree)	Calcite	Aragonite	Vaterite
45.55	14	587	8	46.8	151	19	17
45.6	8	861	9	46.85	233	25	12
45.65	13	828	11	46.9	151	22	8
45.7	14	654	9	46.95	167	29	17
45.75	5	508	9	47	139	21	14
45.8	11	317	19	47.05	92	18	19
45.85	15	177	11	47.1	122	17	21
45.9	16	99	12	47.15	242	23	16
45.95	11	61	15	47.2	718	41	13
46	5	45	15	47.25	1176	83	13
46.05	9	24	11	47.3	737	55	12
46.1	13	24	14	47.35	687	32	17
46.15	13	25	11	47.4	471	44	19
46.2	15	23	15	47.45	197	29	6
46.25	15	29	15	47.5	95	25	14
46.3	15	26	11	47.55	35	24	14
46.35	15	15	13	47.6	33	21	11
46.4	14	21	13	47.65	23	25	13
46.45	22	17	15	47.7	18	36	10
46.5	13	17	9	47.75	20	33	19
46.55	17	17	11	47.8	24	47	11
46.6	21	17	9	47.85	25	66	12
46.65	18	18	19	47.9	19	111	9
46.7	19	19	19	47.95	27	171	11
46.75	56	23	15	48	33	211	17

Table A.7 (Contd.) Data for Figure 4.5 (c) XRD of pure calcium carbonate polymorphs showing characteristic peak of Aragonite 221 at 45.7°.

Angle (degree)	Calcite	20% Vaterite	40% Vaterite	60% Vaterite	80% Vaterite	100% Vaterite
24	21	25	17	23	26	32
24.05	21	23	21	25	29	34
24.1	13	21	23	21	25	35
24.15	12	21	27	25	24	32
24.2	20	18	21	33	32	34
24.25	15	23	27	31	35	33
24.3	18	19	30	35	42	34
24.35	23	22	40	47	74	32
24.4	19	39	64	71	84	57
24.45	21	43	92	128	133	106
24.5	19	93	143	211	252	190
24.55	17	113	196	321	369	348
24.6	16	100	176	261	430	526
24.65	17	77	103	209	451	566
24.7	19	59	75	119	325	367
24.75	15	24	36	81	213	197
24.8	12	17	21	55	103	107
24.85	16	23	23	51	67	54
24.9	18	23	23	37	40	45
24.95	15	18	27	31	31	33
25	19	13	27	29	30	24
25.05	9	15	20	18	24	33
25.1	17	19	21	21	33	26
25.15	11	19	18	18	18	25
25.2	13	19	21	22	23	26
25.25	19	13	19	18	21	33
25.3	14	17	21	24	21	29
25.35	13	15	18	24	19	29
25.4	12	17	17	23	19	31
25.45	16	11	15	18	21	22
25.5	19	19	15	27	23	29
25.55	19	16	19	20	26	30
25.6	17	13	16	19	25	25
25.65	19	19	23	13	26	26
25.7	7	15	17	16	23	31

Table A.8 Data for Figure 4.6 (a) XRD pattern of mixtures of pure calcite and vaterite showing the variation in peak intensity due to diffraction by 110 plane at 24.6° as a function of vaterite concentration.

Angle (degree)	Calcite	20% Vaterite	40% Vaterite	60% Vaterite	80% Vaterite	100% Vaterite
28.5	21	19	14	26	19	23
28.55	21	24	16	27	19	18
28.6	25	30	18	21	25	28
28.65	31	23	29	27	26	21
28.7	30	36	24	28	21	27
28.75	35	28	30	32	22	13
28.8	76	51	37	37	29	15
28.85	114	71	70	27	37	19
28.9	243	194	109	67	51	23
28.95	491	356	245	147	71	22
29	1284	567	694	419	113	27
29.05	1647	1477	1520	763	354	28
29.1	2019	1921	1678	831	687	34
29.15	1459	1352	1061	555	719	63
29.2	734	637	482	330	471	33
29.25	300	186	121	165	216	33
29.3	193	66	55	93	84	28
29.35	139	26	26	131	50	17
29.4	69	33	27	189	29	22
29.45	39	19	17	204	31	26
29.5	23	23	17	103	29	35
29.55	17	17	17	49	25	17
29.6	13	17	26	21	26	21
29.65	12	17	19	24	21	19
29.7	16	17	21	24	23	27
29.75	11	10	23	18	24	21
29.8	17	15	13	22	23	23
29.85	13	13	19	19	16	19
29.9	11	12	11	17	17	25
29.95	11	13	12	25	23	13
30	15	19	17	17	14	15
30.05	11	16	15	22	20	26
30.1	11	7	22	18	29	14

Table A.9 Figure 4.6 (b) XRD pattern of mixtures of pure calcite and vaterite showing the variation in peak intensity due to diffraction by 104 plane at 29.1° as a function of vaterite concentration.

Percent vaterite	I_{110} / I_{104}	Standard deviation
20	0.06	0.017
40	0.25	0.035
60	0.39	0.15
80	0.59	0.025
100	0.76	0.032

Table A.10 Data for Figure 4.7 Calibration curve obtained by plotting intensity ratio of 110 and 104 diffraction peaks at 24.6° and 29.1° for XRD pattern of mixtures of pure polymorphs (calcite and vaterite).

Uncontrolled addition		Step addition		Acusol®		PMI_Cu_sys[1]	
Time (min.)	Calcium Conc. (ppm)	Time (min.)	Calcium Conc. (ppm)	Time (min.)	Calcium Conc. (ppm)	Time (min.)	Calcium Conc. (ppm)
25.00	1.00	11.00	0.00	11.50	0.01	16.50	0.01
28.00	2.00	14.00	0.00	15.00	0.01	21.50	0.10
31.00	4.00	17.00	0.00	18.00	0.30	67.00	0.28
34.00	6.00	20.00	0.00	21.00	0.94	69.50	0.30
37.00	8.00	23.00	0.00	29.00	0.99	81.00	0.30
40.00	10.00	26.50	0.00	37.00	1.20	86.00	0.32
43.00	12.00	30.00	0.41	40.50	1.21	93.50	0.35
46.00	14.00	33.00	0.81	45.00	1.22	103.00	0.37
49.00	15.50	46.50	0.94	50.00	1.26	109.00	0.37
52.00	14.00	80.00	0.97	54.00	1.29	119.50	0.43
55.00	12.00	120.00	1.00	59.00	1.31	136.00	0.50
58.00	10.00	150.00	1.00	64.00	1.37	152.50	0.54
61.00	8.25	180.00	1.00	84.00	1.40	155.00	0.63
64.00	8.25	210.00	1.00	104.00	1.41	169.00	0.63
67.00	8.25	239.00	1.01	124.00	1.42	184.50	0.68
70.00	8.25	245.00	1.18	144.00	1.43	186.50	0.73
98.00	8.25	255.50	1.37	164.00	1.46	200.50	0.79
118.00	8.25	269.50	1.59	187.00	1.47	216.00	0.85
138.00	8.25	271.50	2.00	210.00	1.48	218.00	0.99
158.00	8.25	273.50	2.33	246.00	1.50	219.00	1.15
178.00	8.25	287.50	3.41	258.50	1.62	234.00	1.34
198.00	8.25	288.00	3.96	259.00	1.75	248.00	1.44
218.00	8.25	288.50	4.28	260.00	2.04	250.50	1.80
238.00	8.25	297.00	4.98	262.50	2.21	264.00	1.94
258.00	8.25	302.50	5.79	275.00	3.24	265.50	2.62
278.00	8.25	303.00	6.74	276.50	4.09	267.50	2.83
298.00	8.25	303.50	7.28	278.00	5.57	280.00	3.29
318.00	8.25	304.00	8.46	290.00	6.49	281.50	4.78
338.00	8.25	304.50	9.14	290.50	7.58	283.50	5.16
358.00	8.25	305.00	10.64	291.00	8.84	296.00	6.46
378.00	8.25	305.50	11.47	291.50	9.54	297.00	8.71
398.00	8.25	306.50	10.64	292.00	11.15	297.50	10.12
		309.00	9.85	292.50	12.03	298.00	11.76
		313.00	9.14	293.00	14.04	298.50	13.68
		326.50	9.14	293.50	15.17	300.00	15.90

Table A.11 Data for Figure 4.9 Calcium ion concentration during calcium carbonate crystallized in presence of various polymeric additives.

[1] *PMI_Cu_sys* refers to Polymaleimide synthesized by bis(triphenylphosphine) Cu(I) nitrate and t-butyl benzyl alcohol initiator

Polyaspartic Acid		Polyacrylic Acid		PMI Synthesized by PbO Initiator		PMI Synthesized by KOH Initiator	
Time (min.)	Calcium Conc. (ppm)	Time (min.)	Calcium Conc. (ppm)	Time (min.)	Calcium Conc. (ppm)	Time (min.)	Calcium Conc. (ppm)
10.50	0.00	11.00	0.00	16.50	0.00	11.00	0.00
16.50	0.09	16.00	0.00	25.50	0.00	16.00	0.00
17.00	0.25	40.50	0.10	32.50	0.00	19.50	0.02
32.00	0.94	54.00	0.10	38.50	0.00	26.00	0.04
38.50	1.19	65.00	0.12	49.00	0.00	35.00	0.04
48.50	1.37	69.00	0.14	65.00	0.00	50.00	0.08
58.00	1.48	82.00	0.14	81.00	0.00	65.50	0.14
66.00	1.57	85.50	0.15	86.50	0.01	83.50	0.15
73.50	1.74	100.00	0.16	98.50	0.01	102.00	0.17
93.50	1.91	117.00	0.16	115.50	0.01	133.00	0.15
108.00	2.00	131.50	0.18	131.00	0.01	149.50	0.18
118.50	2.12	149.00	0.19	149.00	0.01	165.50	0.23
138.00	2.32	165.50	0.22	179.00	0.02	196.00	0.27
148.00	2.45	179.00	0.24	194.00	0.02	212.00	0.32
168.00	2.44	195.00	0.28	221.00	0.02	229.00	0.34
188.00	2.44	212.50	0.30	226.50	0.03	244.00	0.40
216.00	2.44	226.50	0.36	232.00	0.04	259.50	0.56
230.00	2.44	242.00	0.41	244.00	0.06	275.00	0.72
275.50	2.42	257.50	0.56	259.50	0.08	276.50	0.99
276.00	2.62	267.50	0.66	267.50	0.10	279.00	1.62
276.50	2.84	273.00	0.83	277.00	0.40	279.50	1.76
277.00	3.07	274.00	1.13	287.00	0.70	282.50	2.25
277.50	3.32	275.00	1.42	294.00	1.05	286.50	3.11
279.00	3.89	276.50	1.93	297.00	1.27	287.50	1.27
290.50	4.55	279.50	2.25	315.00	1.30	299.00	1.27
291.50	5.77	289.50	2.84	325.00	1.32	320.00	1.27
292.00	6.75	290.50	3.86	339.50	1.35	340.00	1.27
292.50	7.31	291.50	5.25	354.00	1.47	360.00	1.27
293.00	8.55	292.50	6.61	364.00	1.60	380.00	1.27
293.50	9.26	293.50	8.33	374.00	1.60	400.00	1.27
294.00	10.84	294.00	9.71	384.00	1.60		
295.00	10.02	297.00	9.00	399.50	1.60		
297.00	9.26	299.00	8.33				
298.50	8.55	304.50	8.33				

Table A.11 (Contd.) Data for Figure 4.9 Calcium ion concentration during calcium carbonate crystallized in presence of various polymeric additives.

Time (min.)	Percent Vaterite					
	Acusol®	PaspAcid[1]	PAA[2]	PMI_KOH[3]	PMI_PbO[4]	PMI_Cu_sys[5]
290	100	2.50	1.42	1.80	0	2.10
305	100	15.50	34.51	3.80	0	13.50
315	100	31.20	45.70	6.70	0	27.50
325	100	45.10	65.22	9.80	0	32.50
335	100	48.30	92.51	12.30	0	35.60
345	100	49.40	99.09	14.90	0	37.80
355	100	51.50	99.09	15.60	0	41.30
365	100	51.50	99.09	17.70	0	43.20
375	100	51.50	99.09	19.30	0	45.90
385	100	51.50	99.09	19.30	0	45.90
395	100	51.50	99.09	19.30	0	45.90
405	100	51.50	99.09	19.30	0	45.90
415	100	51.50	99.09	19.30	0	45.90

Table A.12 Data for Figure 4.10 Percent vaterite during calcium carbonate crystallized in presence of various polymeric additives by Raman spectroscopy.

[1] *PAspAcid* refers to Polyaspartic acid
[2] *PAA* refers to Polyacrylic acid
[3] *PMI_KOH* refers to Polymaleimide synthesized by KOH initiator
[4] *PMI_PbO* refers to Polymaleimide synthesized by PbO and t-butyl benzyl alcohol initiator
[5] *PMI_Cu_sys* refers to Polymaleimide synthesized by bis(triphenylphosphine) Cu(I) nitrate and t-butyl benzyl alcohol initiator